AWARD NUMBER: W81XWH-18-1-0519

TITLE: Early Detection of Castration-Resistant Prostate Cancer by Assessing Interactions Between Circulating Tumor Cells and Accompanying Immune Cells

PRINCIPAL INVESTIGATOR: Tim H. Huang, Ph.D.

CONTRACTING ORGANIZATION: The University of Texas Health Science Center at San Antonio, Texas 78229

REPORT DATE: September 2020

TYPE OF REPORT: Annual

PREPARED FOR: U.S. Army Medical Research and Development Command
Fort Detrick, Maryland 21702-5012

DISTRIBUTION STATEMENT: Approved for Public Release;
Distribution Unlimited

The views, opinions and/or findings contained in this report are those of the author(s) and should not be construed as an official Department of the Army position, policy or decision unless so designated by other documentation.

REPORT DOCUMENTATION PAGE

Form Approved
OMB No. 0704-0188

Public reporting burden for this collection of information is estimated to average 1 hour per response, including the time for reviewing instructions, searching existing data sources, gathering and maintaining the data needed, and completing and reviewing this collection of information. Send comments regarding this burden estimate or any other aspect of this collection of information, including suggestions for reducing this burden to Department of Defense, Washington Headquarters Services, Directorate for Information Operations and Reports (0704-0188), 1215 Jefferson Davis Highway, Suite 1204, Arlington, VA 22202-4302. Respondents should be aware that notwithstanding any other provision of law, no person shall be subject to any penalty for failing to comply with a collection of information if it does not display a currently valid OMB control number. **PLEASE DO NOT RETURN YOUR FORM TO THE ABOVE ADDRESS.**

1. REPORT DATE	2. REPORT TYPE	3. DATES COVERED
SEPTEMBER 2020	Annual	8/15/2019-8/14/2020

4. TITLE AND SUBTITLE

Early Detection of Castration-Resistant Prostate Cancer by Assessing Interactions Between Circulating Tumor Cells and Accompanying Immune Cells

5a. CONTRACT NUMBER
W81XWH-18-1-0519

5b. GRANT NUMBER
PC170821

5c. PROGRAM ELEMENT NUMBER

6. AUTHOR(S)
Tim H. Huang, PhD
Maria Gaczynska, PhD
Pawel Osmulski, PhD

E-Mail:huangt3@uthscsa.edu

5d. PROJECT NUMBER

5e. TASK NUMBER

5f. WORK UNIT NUMBER

7. PERFORMING ORGANIZATION NAME(S) AND ADDRESS(ES)
The University of Texas Health Science Center at San Antonio
Office of Sponsored Programs
7703 Floyd Curl Drive,MC 7828
San Antonio, TX 78229-3900

8. PERFORMING ORGANIZATION REPORT NUMBER

9. SPONSORING / MONITORING AGENCY NAME(S) AND ADDRESS(ES)

U.S. Army Medical Research and Development Command
Fort Detrick, Maryland 21702-5012

10. SPONSOR/MONITOR'S ACRONYM(S)

11. SPONSOR/MONITOR'S REPORT NUMBER(S)

12. DISTRIBUTION / AVAILABILITY STATEMENT

Approved for Public Release; Distribution Unlimited

13. SUPPLEMENTARY NOTES

14. ABSTRACT

Prostate cancer is the most frequently diagnosed cancer in men. In majority of "castration sensitive" patients proliferation of cancer cells depends on supply of androgen and can be attenuated by the androgen deprivation therapy(ADT). Unfortunately, many patients develop "castration resistance"(CR), when the tumor growth and metastatic spread continue despite ADT. For effective second-line therapy the resistance needs to be detected early. Circulating tumor cells(CTCs) that can be isolated from the standard blood sample are considered "seeds of metastasis". We postulate that mechanical and immunochemical profiling of CTCs and accompanying immune cells provide clues about CTCs aggressiveness and the risk of Cr. Our specific aims call for determining the role of (1) epithelial-mesenchymal_transition(EMT) and (2) interactions with circulating macrophages in survival-promoting mechanical fitness of CTCs. Combing the cell culture studies with profiling of CTCs will lead to (3)construction of predictive model for early CR detection. In this reporting period we continued accrual of patients, unfortunately temporarily halted by the COVID-19 Pandemic measures. The accrual and sample collection fully resumed this summer. We performed cell culture experiments and analyzed the data in accordance with the statement of work, with some tasks completed ahead of schedule. We performed initial analyzes of cumulative patients' data. The outcome includes a manuscript submitted.

15. SUBJECT TERMS
androgen deprivation therapy, atomic force microscopy, castration resistance, castration sensitivity, circulating tumor cells, cultured cells, epithelial-mesenchymal transition

16. SECURITY CLASSIFICATION OF:			17. LIMITATION OF ABSTRACT	18. NUMBER OF PAGES	19a. NAME OF RESPONSIBLE PERSON
a. REPORT	b. ABSTRACT	c. THIS PAGE			USAMRMC
Unclassified	Unclassified	Unclassified	Unclassified	59	19b. TELEPHONE NUMBER *(include area code)*

Standard Form 298 (Rev. 8-98)
Prescribed by ANSI Std. Z39.18

TABLE OF CONTENTS

1. Introduction

Prostate cancer (PCa) is the most frequently diagnosed cancer in men. In majority of "castration sensitive" patients proliferation of cancer cells depends on supply of androgen and can be attenuated by the androgen deprivation therapy (ADT). Unfortunately, many patients develop "castration resistance" (CR), when the tumor growth and metastatic spread continue despite ADT. For effective second-line therapy that saves lives and improves life quality the resistance needs to be detected early. To reach the goal of early detection we propose to test properties of rare cells that are responsible for spreading metastasis. These circulating tumor cells (CTCs) are shed from the primary tumor or metastatic lesions and can be isolated from the standard blood sample are considered "seeds of metastasis". Majority of CTCs die, however the surviving "aggressive" cells travel with blood, undergo epithelial-to-mesenchymal transition (EMT), extravasate and start secondary tumor growth in distant organs. Since CTCs have to escape from the tumor and then survive in the turbulent blood stream, they have to be mechanically fit. Indeed, we found in retrospective studies that CTCs obtained from CR patients are much softer, deformable and more adhesive than CTCs from CS patients. CTCs are often accompanied by innate immune cells, mostly macrophages. We found that interactions with macrophages of certain polarization may help CTCs to survive. We postulate that mechanical and immunochemical profiling of CTCs and co-purifying immune cells (tumor associated circulating cells; TACCs) provide clues about CTCs aggressiveness and the risk of CR. Our specific aims call for determining the role of (1) epithelial-mesenchymal transition and (2) interactions with circulating macrophages in survival-promoting mechanical fitness of CTCs. Combining the cell culture studies with profiling of CTCs will lead to (3) construction of predictive model for early CR detection. According to the Statement of Work (SOW), our goals for this reporting period (months 13-24) were: (a) continuation of accrual of patients starting ADT; (b) isolation, enumeration, mechanical and molecular profiling as well as immunochemical characterization of TACCs from the patients' blood; (c) recapitulation of CTC-macrophage interactions in cell culture model: co-culturing of model "CTCs" (prostate cancer cell lines) with model polarized macrophages; the experiments include mechanical and molecular profiling of control and co-cultured "CTCs"; (d) comparing the clinical and biophysical/molecular data for available patient samples.

2. Keywords

androgen deprivation therapy

atomic force microscopy

castration resistance

castration sensitivity

cell adhesion

cell deformation

cell stiffness

circulating tumor cells

cultured cells

epithelial-mesenchymal transition

gene expression

immune cells

immunostaining

liquid biopsy

macrophage

macrophage polarization

mass cytometry

mechanical phenotype

metastasis

prostate cancer

protein expression

single-cell profiling

3. Accomplishments

3.1 The major goals for the first and second reporting periods (months 1-24) and ahead-of-schedule tasks, as stated in the approved SOW, with % of completion.

Research-Specific Tasks:

Specific Aim 1: We will determine the role of epithelial to mesenchymal transition in mechanical fitness of CTCs.	**Months**	**Participants**	**% completion (mo. 13-24)**
Major Task 1: Recruit post-castration metastatic PCa patients experiencing biochemical recurrence and starting first line ADT	4-26	Drs. Huang, Liss	66
Major Task 2: Isolate and immunostain TACCs from the samples of blood drawn from the patients right before the start of ADT (70 patients, time t0), enumerate CTCs.	4-28		48
Subtask 1: Perform microfiltration, immunostain the cells. Device for cell isolation: ScreenCell CC ha (ScreenCell)	4-26	Drs. Osmulski, Gaczynska, Chen,	66
Subtask 2: Enumerate the isolated and immunostained CTCs and classify them as $EpCAM^{+}$ or EMT-CTCs according to surface antigen expression.	4-26	Drs. Gaczynska, Osmulski	30
Major Task 3: Collect multiparameter nanomechanical and morphological data on individual isolated CTCs using PeakForce Quantitative Nanomechanics (PF QNM) AFM imaging	4-30		45
Subtask 1: Collect the AFM images.	4-26	Drs. Osmulski, Gaczynska	66
Subtask 2: Perform image and data analysis on the collected AFM images.	4-30	Drs. Osmulski, Gaczynska	33
Major Task 4: Perform the gene expression analysis on CTCs.	4-26		100

Major Task 5: Recapitulate EMT in cell culture model	6-24		90
Subtask 1: Culture 22Rv1 and DU145 cells (source: ATCC) according to ATCC recommendations. Induce EMT by treatment with TGF-β._ _Perform mechanical phenotyping of selected cultured cells.	6-18	Drs. Osmulski, Gaczynska	100
Subtask 2: Perform gene expression analysis of cultured cells that were mechanically phenotyped.	6-18	Dr. Chen	30
Specific Aim 2: We will define the role of CTC-macrophage interactions in mechanical fitness of CTCs.			
Major Task 6: Define the functional composition of macrophage population in TACCs preparations isolated from patients' blood. _	1-26		50
Subtask 1: Enumerate and classify non-CTC patient-isolated TACCs according to immunostaining, enumerate CTC-immune cell clusters.	1-24	Drs. Gaczynska, Osmulski	25
Subtask 2: Perform the gene expression analysis on randomly selected cells (up to 30) bearing immune cell markers.	1-32	Dr. Chen	100 (ahead)
Major Task 7: Recapitulate the interactions of model "CTCs" (prostate cancer cell lines) cultured with polarized macrophages.	12-30		100 (ahead)
Subtask 1: Co-culture 22Rv1 and DU145 cells with model macrophages derived from U937 cells (source: ATCC). Determine rates of growth of co-cultured cells, enumerate cell clusters.	12-24	Drs. Gaczynska, Osmulski	100
Subtask 2: Perform mechanical phenotyping of selected cultured cells, free or in clusters.	12-24	Drs. Gaczynska, Osmulski	100

Subtask 3: Perform the gene expression analysis on model CTCs and macrophages.	12-30	Dr. Chen	100 (ahead)
Specific Aim 3. We will construct a model for patients' stratification predicting the risk of castration resistance based on the mechanical fitness of CTCs.			
Major Task 8: Collect mechanical and immunocytochemical properties of TACCs isolated at time t1 (6 months or at failure)	6-30		22
Subtask 1: Perform microfiltration, immunostain the cells, enumerate as for t0.	6-30	Drs. Gaczynska, Osmulski	22
Subtask 2: Perform mechanical profiling of CTCs at time t1, perform image and data analysis on the collected AFM images as for t0.	6-30	Drs. Gaczynska, Osmulski	22
Subtask 3: Compare clinical and biophysical/gene expression data at t1	6-30	Drs. Huang, Liss, Gelfond, Osmulski, Gaczynska	22

3.2 Specific accomplishments under the Major Tasks listed above:

3.2.1 Specific Aim 1, Major Task 1

We planned to accrue a total of 70 metastatic prostate cancer patients starting first-line ADT. During the first 12 months of the project duration we accrued a total of 38 patients (54%), the on-target number. Unfortunately, the COVID-19 pandemic caused a five-months hiatus in accrual, from the end of February to the end of July. The accrual process resumed in August and we expect to finish it with a delay accommodating the pandemic measures.

Table 1 presents the accrual numbers, with information on data collected, relevant for Major Tasks 1-4, 6 and 8, total and specifically in the current reporting period (period 2; 08/15/2019 – 08/14/2020).

Number	Total	This reporting period	Total 1st visit (t0)	Total two visits (t0 and t1)
Patients (PTs) accrued	**46**	**8**	**31**	**15**
PT samples with TACCs Collected for Mechanical and Immunochemical Phenotyping	61	12	31	30
TACCs Retained on Filters (approximately)	9000	2000	4600	4400
PT Samples Mechanically Phenotyped	61	12	31	30
PT Samples with Mechanical Phenotype Analyzed	46	26	16	30
CTCs with Mechanical Phenotype Collected	1022	238	511	511
CTCs with Mechanical Phenotype Analyzed	679	375	220	459
PT Samples with Immunostaining Performed and Cell Images Collected	61	12	31	30
Immunostaining Images Collected	2363	1423	1165	1198
PT Samples with TACCs Enumeration Completed	29	15	7	22
PT Samples with Cells Collected for Gene and Protein Expression Analysis	61	12	31	30
PT Samples with TACCs analyzed by single-cell transcriptomics	20	10	20	0
CTCs analyzed by single-cell transcriptomics	273	137	273	0
Immune cells analyzed by single-cell transcriptomics	143	143	143	0

3.2.2 Specific Aim 1, Major Task 2

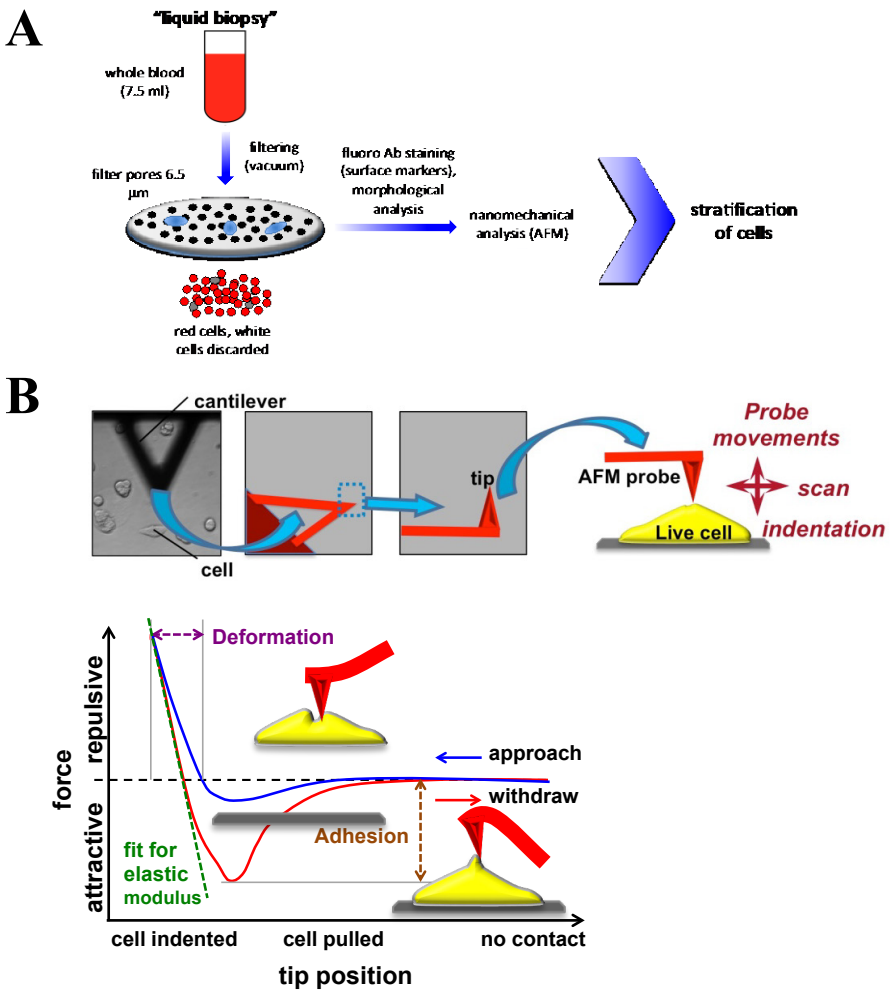

Figure 1 Processing of liquid biopsy samples from prostate cancer patients (as in report period 1).
A: isolation of large tumor associated circulating cells (TACCs). A separate filter is used to collect additional TACCs for gene and protein expression analysis. **B**: nanomechanical profiling: a small silicon probe on a cantilever "pokes" the cell with extremely small (nanoNewton-scale) force to collect "force curves" used to extract precise numerical data on elasticity (reversible change of shape), deformability (reversible and non-reversible, nondestructive change of shape) and adhesiveness.

For all blood samples we collected filters with retained cells and images of immunostained TACCs (*Subtask 1*). The patient's blood samples were processed within two hours from phlebothomy, as planned. Processing included microfiltration with the ScreenCell device retaining all cells that do not pass through 6.5 µm pores randomly distributed in the filters. The filters are formulated for cells' adherence, important to hold cells for AFM profiling. The cells still attached to the filters are subjected to nanomechanical imaging. The methods of processing

and AFM imaging did not change since the last reporting period and are presented above in **Figure 1.**

All large cells collected on filters are immunostained and photographed for enumeration and classification. To date, we fully enumerated and classified CTCs for nearly half of collected samples (*Subtask 2*). See **Table 1** for details. Analysis of correlations of enumeration of distinct classes of CTCs and mechanical phenotypes of CTCs is presented below, with a progress report for *Specific Aim 1, Major Task 3.*

3.2.3 Specific Aim 1, Major Task 3

Mechanical phenotypes of single CTCs were collected with atomic force microscopy (AFM) PeakForce Quantitative Nanomechanical mode for all collected samples immediately after microfiltration, as planned (*Subtask 1*). As for now, the collected data are fully processed and analyzed for a total of 46 samples, which accounts for 75% of all samples collected for the project to date (*Subtask 2*; see **Table 1** for details). For all analyzed CTCs, a full mechanical phenotype with cell elasticity, deformation and adhesion, was collected. **Figure 2** presents an example of AFM-collected topography and mechanical phenotype maps of a single CTC.

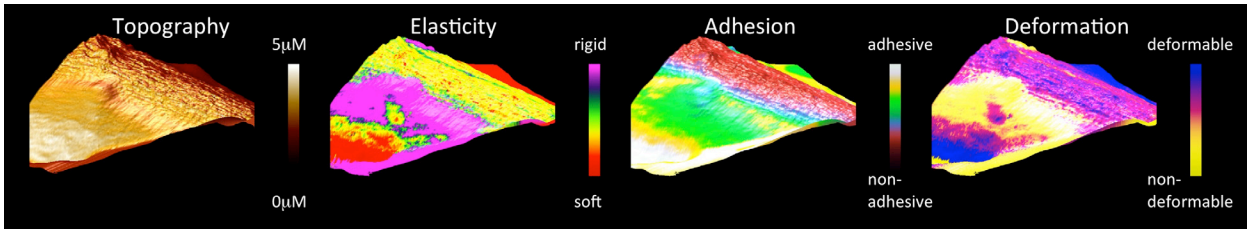

Figure 2 PeakForce Quantitative Nanomechanics (PF-QNM) AFM imaging delivers nanomechanical phenotype o circulating tumor cells. The fragment of a single CTC presented here was characterized by morphological and nanomechanical parameters. Pseudo-3D renderings of maps are colored according to the cell's height (topography), softness, adhesiveness and deformability.

With the mechanical and immunochemical phenotypes analyzed for a significant number of patient samples, we attempted to classify the expectedly diverse cells from a subset of 23 patients (*Subtask 2*). **Figure 3** presents the classification of 514 CTCs isolated from 33 samples. The samples included t0 visits for 13 patients and both t0 and t1 visits for 10 patients. Mechanical phenotypes of 15 to 20 CTCs were collected for each sample. We identified four classes of CTCs, from poorly fit stiff and non-adhesive class 1, to moderately fit class 2 and finally to well fit classes 3 and 4, with exceptionally soft (class 3) and exceptionally adhesive cells (class 4). In **Figure 4** the samples are ordered according to relative abundance of best-fit CTCs (classes 3 and 4). Below the "CTC fitness chart" we present relative partition of CTCs phenotyped according to surface markers, EpCAM and vimentin. Apparently, contribution of typical $EpCAM^+$ CTCs decreased with the increasing fitness of CTC population. This trend was also striking when enumeration of cells was considered rather than relative contribution: enumeration of EMT CTCs ($EpCAM^-$/$vimentin^+$) remained stable along the "mechanical fitness

axis", whereas counts of EpCAM^{+} CTCs systematically decreased (**Figure 4**, right). Nevertheless, we hypothesize that contribution of vimentin^{+} CTCs may actually increase along the "mechanical fitness axis". The EpCAM^{+}/vimentin^{+} cells are now included in the "typical CTC" count, not in the CTC EMT count. Such classification is justified by the established methods of CTC isolation that select CTCs solely on the basis of EpCAM expression (and lack of immune cell markers). Our results clearly point at the shortcomings of EpCAM based CTC isolation/enumeration methods, neglecting diversity of these EMT-undergoing cells.

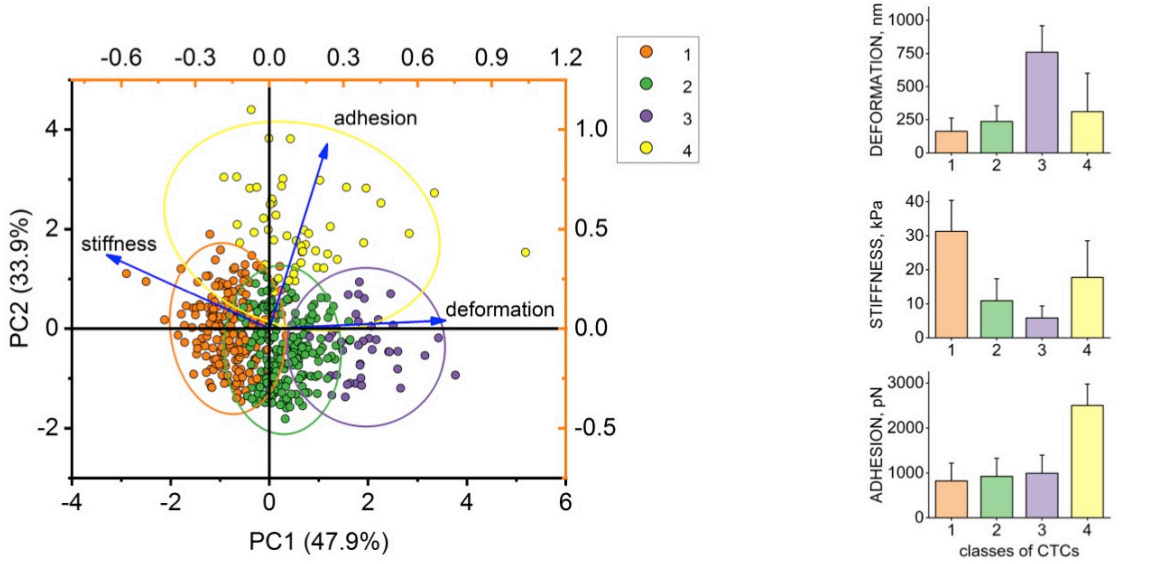

Figure 3 Phenotypical diversity of 514 CTCs isolated from 33 blood samples from 23 patients. Principal component analysis (PCA; left) reveals the presence of four classes of cells with distinct mechanical phenotypes (right). Cell classes were identified with the unsupervised hierarchical clustering. Class 3 and 4 contain the softest and most adhesive cells, respectively, that we consider the most "mechanically fit" to withstand mechanical stress in the bloodstream, survive and proceed with extravasation and seeding metastasis.

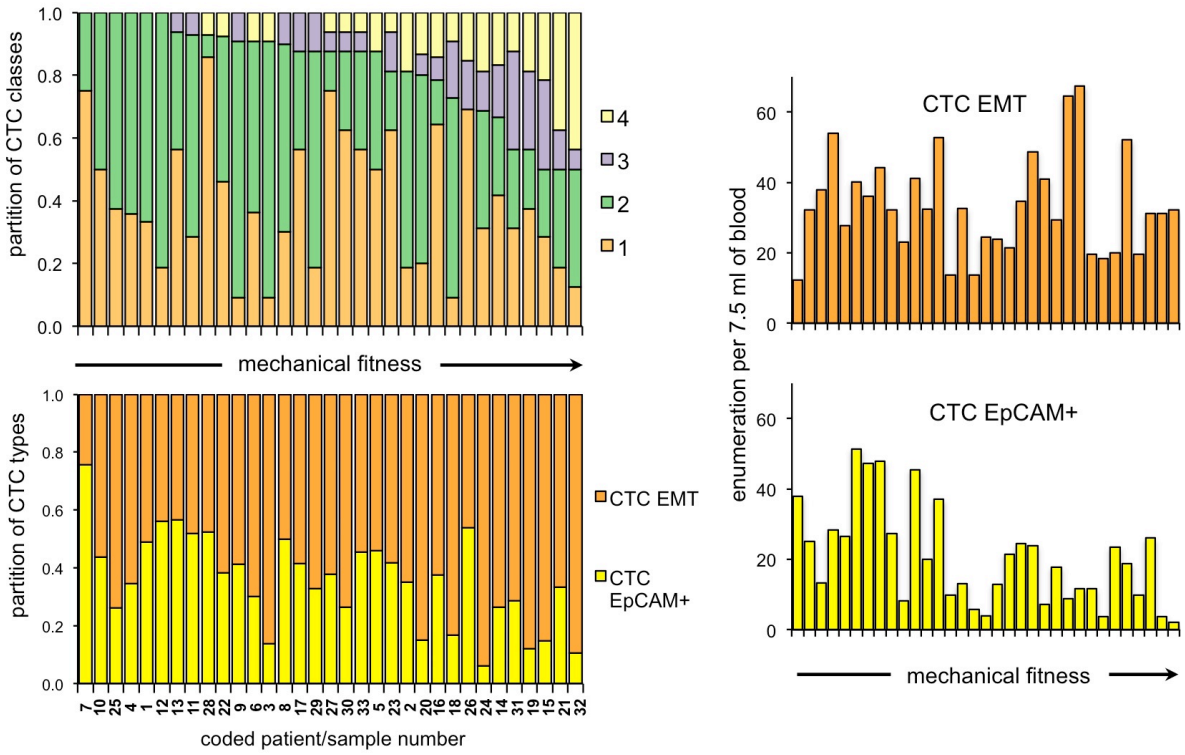

Figure 4 "CTC fitness chart" of prostate cancer patients. Each column represents data for CTCs isolated from a single blood sample. The samples are ordered according to relative abundance of CTCs belonging to mechanical class 4 and 3 (best-fit cells; color coding of classes as in Figure 3). Left-top: relative abundance of the four classes of CTCs. Left-bottom: relative abundance of CTCs phenotyped by their surface markers. Right: enumeration (cells per 7.5 ml of blood) of $EpCAM^+$ CTCs and EMT CTCs ($EpCAM^-$/$vimentin^+$). The samples are ordered as in CTC fitness chart on the left.

3.2.4 Specific Aim 1, Major Task 4

Sets of TACCs have been collected from the patients' samples and preserved for molecular analysis. In this reporting period we analyzed additional 137 large cells (10 patients) negative for immune cell markers, which brings the total number of molecularly characterized CTCs to 273. Transcriptomic expression profiles collected in the previous reporting period revealed high expression of EMT related genes, as expected. The trend was preserved in the new set of CTCs, accompanied by expression of genes important for cancer cells survival (for example: WNT5a), clustering, especially important for CTCs (JUP/plakoglobin) or invasion (SPARC, MMP-9). A heat map of gene expression analysis for CTCs and co-purifying large immune cells (macrophages) is presented below with the progress report for *Specific Aim 2, Major Task 6, Subtask 2*.

To broaden the scope of our analysis we performed mass cytometry (CyTOF) studies on 594 CTCs isolated from additional 8 patients. This time, we isolated large cells from the blood by Ficoll separation and separated them according to leukocyte, epithelial and prostate cell markers (**Figure 5A**). Expectably, we found abundant leukocytes and presumed CTCs positive

for epithelial and prostate markers but negative for immune markers (**Figure 5B-E**). Interestingly, there was also a class of cells with high expression of immune as well as prostate (PSA, PSMA) and epithelial (Muc-1) markers - possibly products of fusion between CTCs and macrophages ("tumacrophages") (**Figure 5E-G**). Interestingly, markers related to energy metabolism, including the transcription regulator menin, indicated that CTCs from patients with higher disease burden (biochemical recurrence/BCR, castration resistance/CR, metastasis) had elevated OXPHOS (oxidative phosphorylation) function, as compared to CS and non-metastatic patients (**Figure 5H**). Efficient OXPHOS promotes survival of cancer cells deployed to circulation and deprived of protective tumor environment.

We consider this task completed. The data will be used alongside the cumulative mechanical phenotypes of CTCs from selected patients. We expect that EMT genes will be upregulated in CTCs of patients with high contribution of well-fit CTCs. As we declared in the previous progress report, we plan to perform an exceptionally effective multi-parameter mass cytometry (CyTOF) analysis for selected CTCs isolated from the incoming patient samples, for additional insight on metabolic pathways involved in mechanical fitness and survival.

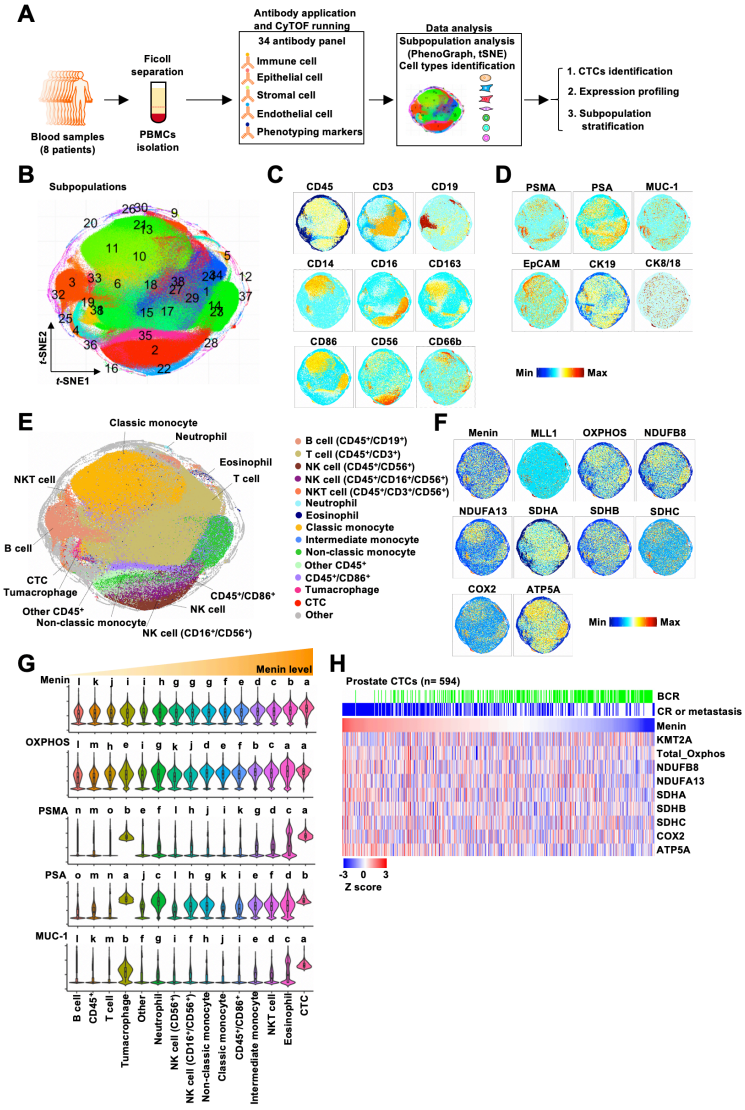

Figure 5 Mass cytometry analysis of CTCs and leukocytes from prostate cancer patients.
A, Schematic workflow of PBMCs processing and mass cytometry (CyTOF). **B,** 38 subpopulations were identified by Phenograph algorithm and visualized in tSNE plot. **C,** Leukocyte markers were displayed by tSNE plots. **D,** Prostate cell markers and epithelial markers were displayed by tSNE plots. **E,** Cell types were identified based on leukocyte, prostate and epithelial markers and displayed by tSNE plot. **F,** Expression profile of menin (OXPHOS promoting transcription factor) and OXPHOS related proteins displayed by tSNE plots. **G,** Menin, OXPHOS, PSMA, PSA, and MUC-1 expression level in cell types displayed by violin plots. **H,** Heat map of menin and OXPHOS related proteins in CTCs of CR or metastatic patients and patients with biochemical recurrence (BCR).

3.2.5 Specific Aim 1, Major Task 5

We induced EMT in model prostate cancer cells: 22Rv1 and DU145, and performed mechanical phenotyping of the control and transition-undergoing cells, as declared in *Subtask 1*. Primary tumor (xenograft) derived 22Rv1 cells are moderately invasive and diverse, with androgen receptor splice variant and mixed androgen dependence/independence phenotype. Brain metastasis derived androgen receptor negative DU45 cells are relatively poorly invasive. We decided to add androgen-independent and highly invasive C4-2 cells (LNCaP derived) to the study to account for cells that are already well mechanically fit, with certain phenotypical features of EMT. Together with the data presented in the previous progress report and describing analysis of cells with hybrid EMT induced by fluid shear stress (FSS), we consider the *Subtask 1* completed. The data collected and analyzed during the current reporting period are presented in **Figures 6 and 7**.

First, we finished nanomechanical characterization of the three cell lines and compared their phenotypes to patient-isolated CTCs. Comparison of 40 22Rv1, 47 DU145 and 52 C4-2 cells with 514 CTCs (total 653 cells) revealed that at least subsets of these cultured cells were very similar to CTCs in terms of their nanomechanical phenotypes. The primary tumor-derived 22Rv1 cells turned out to be the most CTC-like (**Figure 6**). The spread of all parameters in control 22Rv1 cells was the largest, likely due to their mixed genetic background (**Figure 6,** left). In turn, high adhesion, about 1000 nN on average, was the most distinctive feature of DU145, as it was more than twice as high as adhesion of 22Rv1 or C4-2 (averages about 400 nN). C4-2 cells were soft and not very adhesive, suggesting mesenchymal-like phenotype expected in highly invasive tumor cells (**Figure 6**, left).

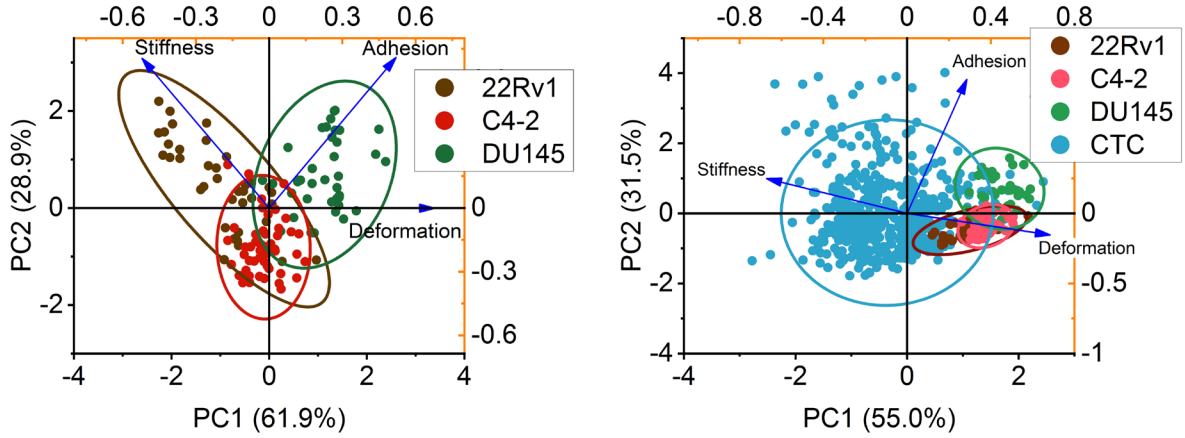

Figure 6 Human cultured prostate cancer cells show mechanical properties specific for each cell line (left). The properties are comparable with patient-isolated CTCs (right). Principal component analysis (PCA) of nanomechanical parameters for 40 22Rv1, 47 DU145 and 52 C4-2 cells with 514 CTCs (total 653 cells) is presented.

Next, we induced EMT in the cultured cells and compared their mechanical parameters to non-induced model controls. We tested distinct conditions for induction to mimic diversity of EMT-prompting physiological settings. The results are presented in **Figure 7**. Mechanical phenotype changes in cultured cells followed the path of canonical EMT: decrease in adhesion

was the most prominent trait, accompanied by a decrease in stiffness and increase in deformability, as expected for cells that forgo sedentary behavior and become mobile. Interestingly, the changes were detectable even in C4-2 cells that already very soft and non-adhesive. However, after a short induction the cells displayed extremely diverse phenotypes. We plan to explore this lead to mimic distinct stages of EMT, including "hybrid EMT".

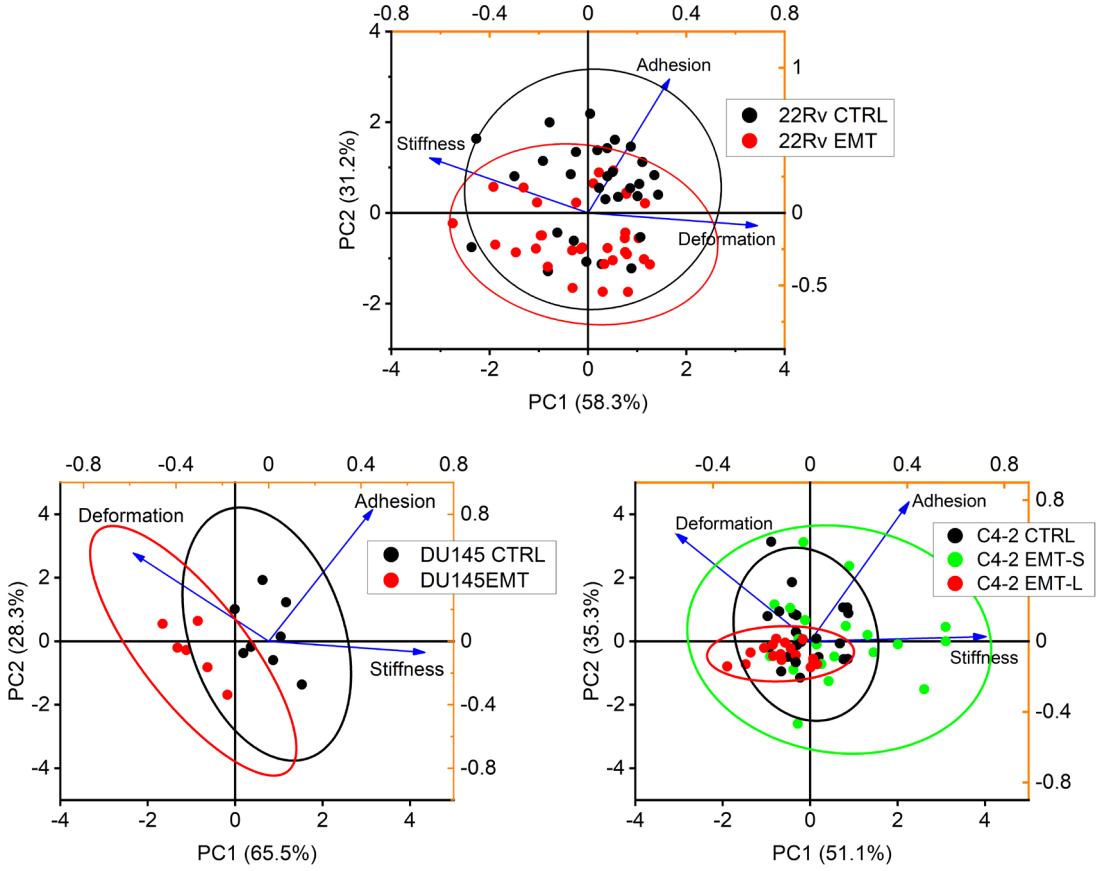

Figure 7 Nanomechanical phenotypes of cultured prostate cancer cells conform to canonical epithelial-to-mesenchymal transition (EMT). 22Rv1 and DU145 cells were induced for 5 days with an EMT-inducing media supplement. C4-2 cells were induced with TGF-beta for one day (short; EMT-S) or one-and a half day (36 hrs; long, EMT-L).

We are collecting cells for mass cytometry (CyTOF) proteomic analysis. The experiments will be performed shortly to complete *Subtask 2* and to finalize the *Major Task 5*.

3.2.6 Specific Aim 2, Major Task 6

The immunostaining-based composition of non-CTC, immune cells population in TACCs (*Subtask 1*) was determined for selected samples, as stated in **Table 1.**

Importantly, we refined our classification of filter-retained large immune cells to recognize "intermediate" macrophages ($CD163^+/CD80^+$; inter-M), which correspond to M2-d type, often found among TAMs (tumor-associated macrophages). This class was before included in M2-like type, which now consists only of $CD163^+/CD80^-$ cells. We hypothesize that macrophages among TACCs prominently (exclusively?) include TAMs released from a tumor, and that inter-Ms are their most typical representation. As a next step, we attempted to search for associations between mechanical phenotypes of CTCs and abundance and composition of co-isolating macrophages. **Figure 8** presents relative abundance and enumeration data for macrophages in patients' samples ordered according to mechanical fitness of CTCs (compare with **Figure 4**). Apparently, the relative abundance of macrophages increased along the axis, at the expense of abundance of CTCs (**Figure 8**, left). Then, the total count of macrophages as well as enumeration of M1-like and intermediate macrophages, increased with increasing partition of well fit CTCs in the patients' samples (**Figure 8**, right). Enumeration of all TACCs presented a weak increasing trend (**Figure 8**, right).

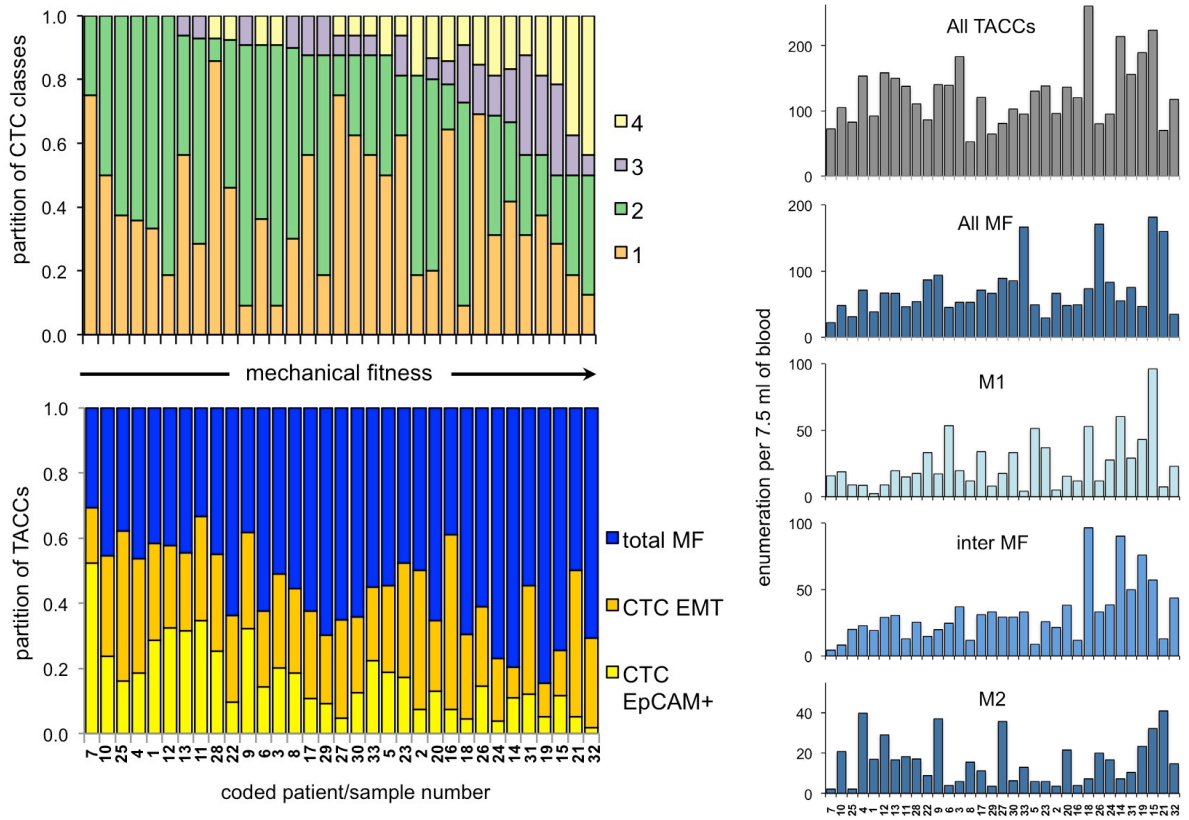

Figure 8 Abundance of macrophages, especially of inter-M and M1 –like phenotypes, increases along the "CTC fitness axis". The 33 samples are ordered according to relative abundance of well-fit CTCs (see Figure 3). Left-top: the "CTC fitness chart" is copied from Figure 4 as a reference. Left-bottom: relative abundance of distinct TACCs. Right: enumeration of all TACCs, and distinct classes of macrophages.

In a search for a formal representation of the trends, we turned to general linear regression analysis. We translated the partition of mechanical phenotype classes (**Figure 4**) into enumeration of the classes in the total CTC population. The strongest correlations are presented

in **Figure 9**. Apparently, enumeration of class 3 with well-fit, very soft cells (**Figure 4**) correlated with enumeration of intermediate macrophages (**Figure 9A**). In turn, enumeration of class 2 with moderately fit cells (**Figure 4**) correlated with enumeration of M2 macrophages (**Figure 9B**). We may speculate that cells from this class were coached specifically by M2 macrophages to attain fitness. Enumeration of well-fit, soft and very adhesive cells from class 4 (**Figure 4**) only weakly correlated with enumeration of M1 (**Figure 9C**) and intermediate macrophages (**Figure 8D**). Possibly these CTCs were already in sufficiently good condition and did not strongly depend on the presence of macrophages for survival. Enumeration of the poorly fit class 1 (very stiff cells; **Figure 4**) did not significantly correlate with any macrophage enumerations (data not shown). These cells were likely destined for apoptosis without evidence of positive or negative intervention from macrophages. Analysis of the trends and correlations will be continued for incoming patients' samples. Even with the limited number of patients-samples, our data suggest a positive correlation between mechanical fitness of CTCs and abundance of macrophages.

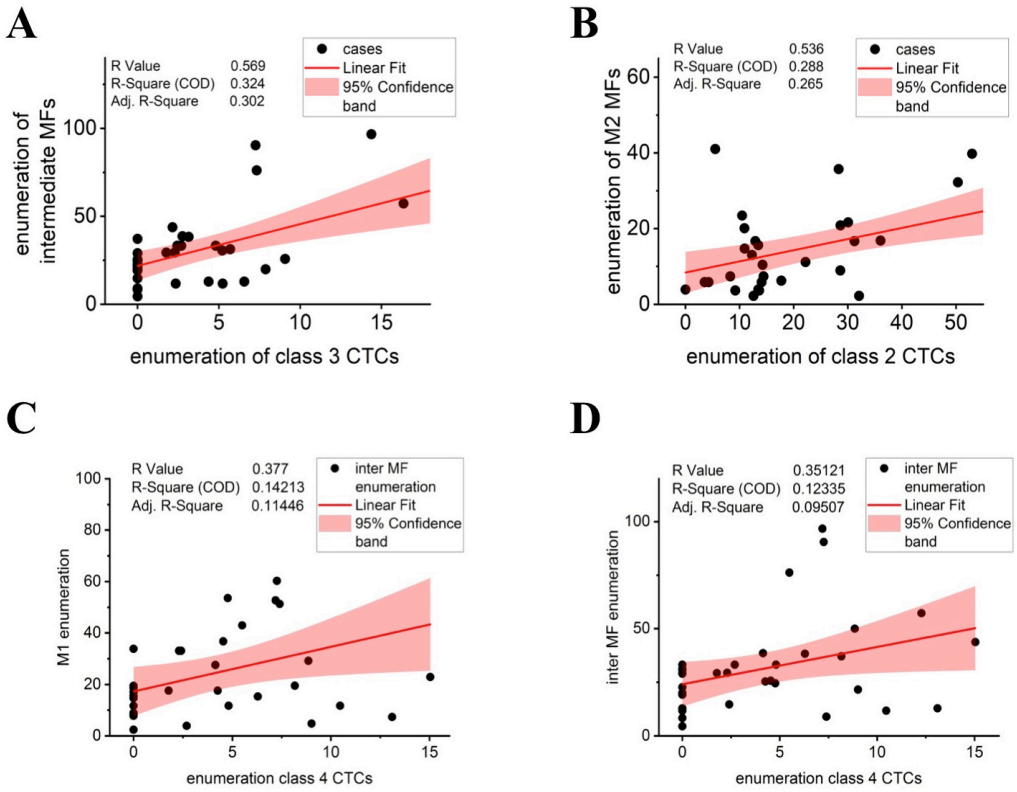

Figure 9 Abundance of well-fit CTCs positively correlates with enumeration of macrophages. Correlations for: **A.** well mechanically fit CTCs (class 3; see Figure 3) and intermediate macrophages; **B.** moderately fit (class 2) CTCs and M2-like macrophages; **C.** well mechanically fit CTCs (class 4) and M1-like macrophages; **D.** well mechanically fit CTCs (class 4) and intermediate macrophages (general linear regression).

Correlations between nanomechanical parameters of CTCs and enumerations of macrophages, were also apparent when average elasticity, deformability and adhesion of all

CTCs isolated from a particular blood sample (15-20 CTCs) were considered. As presented in **Figure 10** (top), adhesion of CTCs strongly and positively correlated with enumerations of intermediate macrophages and M1-like macrophages. Highly adhesive CTCs tended to be deformable, as expected for well-fit cells. In turn, highly elastic CTCs (low stiffness) were accompanied by abundant M2-like macrophages (**Figure 10,** bottom). This trait was not followed by highly deformable CTCs, which "preferred" to be accompanied by inter-M (**Figure 10,** bottom). The correlations point at presumably diverse roles for macrophages of distinct polarizations, a lead to explore in future studies. The data presented here and indicating correlations between mechanical phenotypes of CTCs and abundance of TACCs are included in the manuscript submitted to *Cancer Research*.

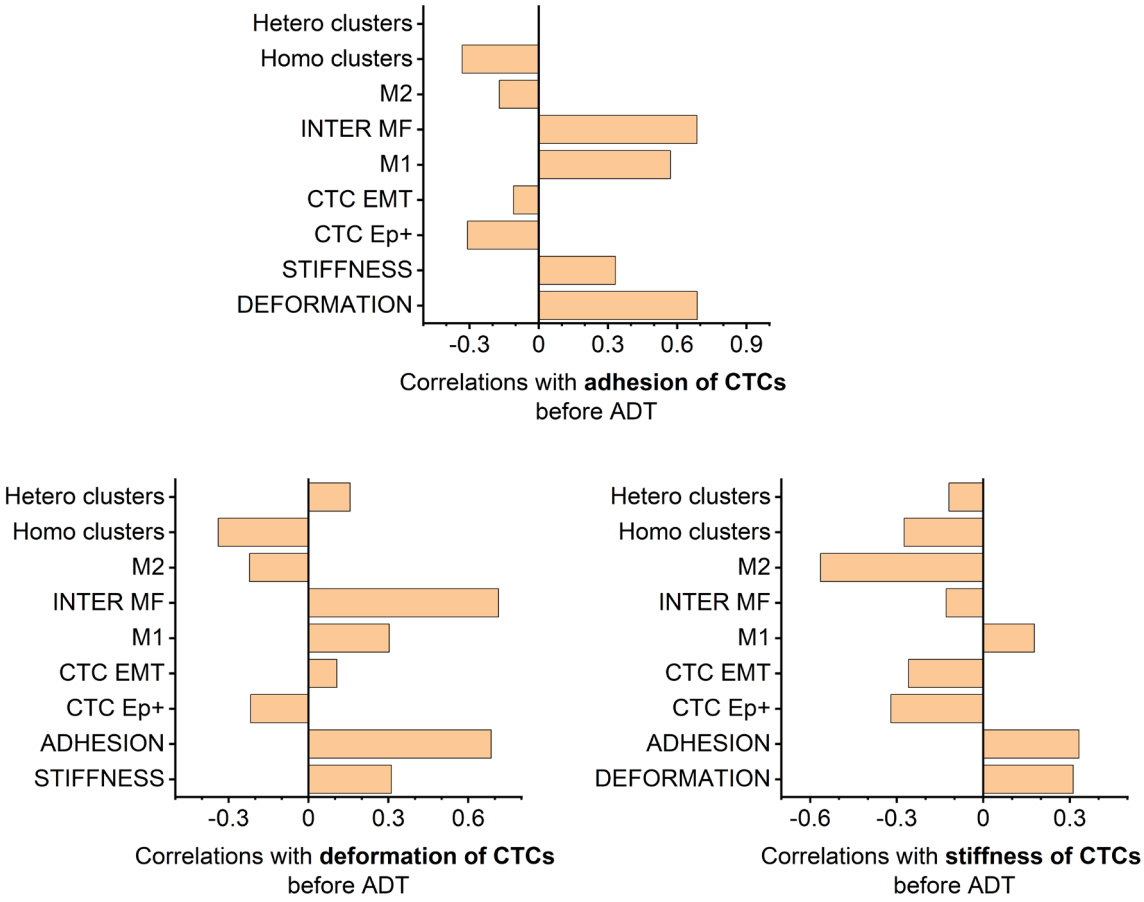

Figure 10 Nanomechanical parameters of patient-isolated CTCs correlate with enumerations of specific types of TACCs, most notably macrophages. Average mechanical parameters for all CTCs isolated from a particular sample and enumerations of TACCs per 7.5 ml of blood are used. "Homo clusters" refer to clusters of CTCs. "Hetero clusters" contain both CTCs and immune cells. Enumerations of CTCs included in the clusters were used for analysis. Data for t0 visits (before ADT) were used for the analysis.

As declared for *Subtask 2* and ahead of schedule, we performed gene expression analysis for spheroids grown from 143 large cells isolated from the patients' blood, negative for EpCAM and positive for immune cell markers. The data, together with gene expression data for spheroids grown from 137 cells bearing CTC markers (pertinent for *Specific Aim 1, Major Task 4* and discussed on Page 13), are presented in **Figure 11**. Expectably, a marker of TAMs, CD163, was prominently expressed. We consider *Subtask 2* completed, with more immune cell analyzed than initially declared (143 rather than 30). The data will be used for the final analysis alongside the cumulative mechanical phenotypes of CTCs from selected patients.

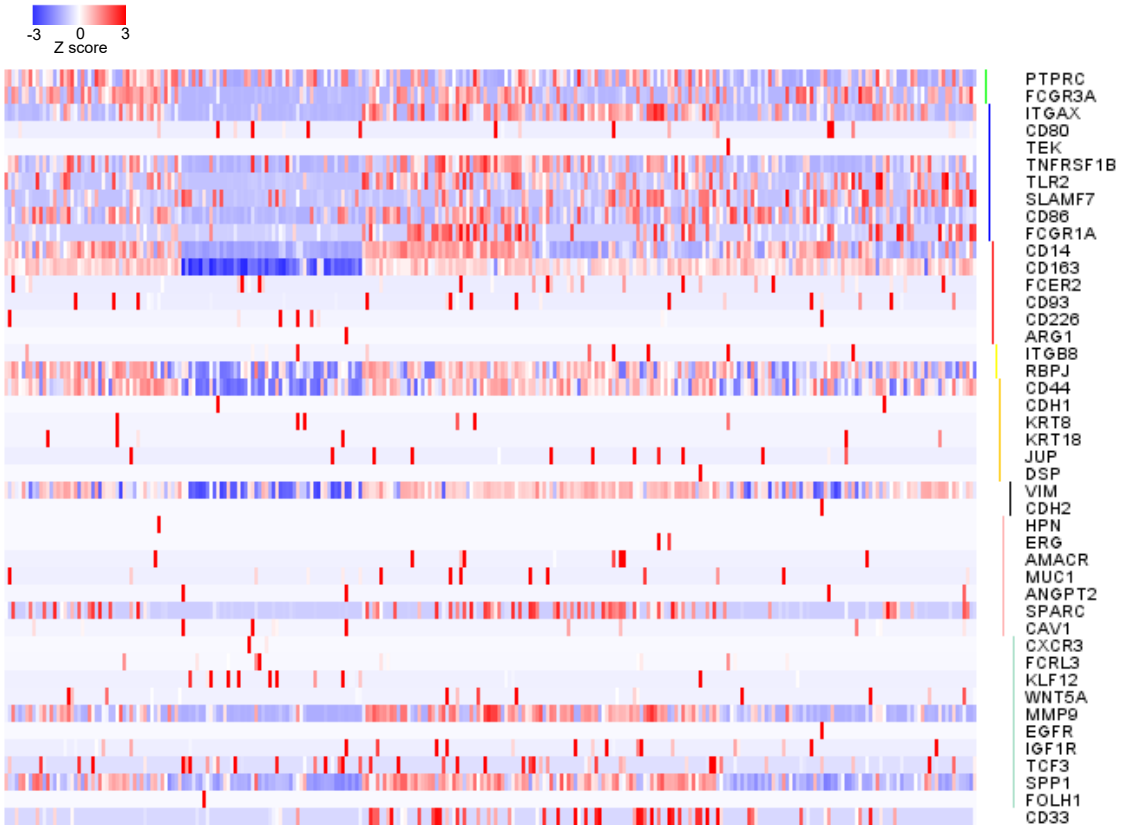

Figure 11 Genes expression in spheroids grown from large cells from the blood of prostate cancer patients indicates the presence of both CTCs and immune cells. Heat map of gene expression is presented. High-low expression is represented by red-blue color scale. 137 spheroids representing CTCs and 143 spheroids representing immune cells were analyzed. The gene list is presented on the right, with immune-related genes listed on the top and followed by genes related to CTCs.

3.2.7 Specific Aim 2, Major Task 7

Recapitulation of the interactions between model CTCs (prostate cancer cell lines) and model macrophages was completed ahead of schedule (all three *Subtasks*). The data are presented below and are included in the manuscript submitted to *Cancer Research*.

As in the case of EMT cell culture model (*Major Task 5*), we included three distinct prostate cancer cell lines into the analysis, with C4-2 cells as an addition to 22Rv1 and DU145 cells declared in *Major Task 7, Subtasks 1 and 2*. Full characterization of nanomechanical phenotypes of the control cultured cells, and comparison of the phenotypes with patient-isolated CTCs is presented and discussed above (**Figure 6**). Summarizing, cultured cells presented nanomechanical profiles comparable with CTCs, albeit more extreme than majority of CTCs: 22Rv1 and especially C4-2 were softer, whereas DU145 were more adhesive than patient-isolated cells (**Figure 6**). Comparing the mechanical parameters between the three cell lines, control 22Rv1 cells were of moderate and variable adhesion, stiffness and deformation, DU145 were very deformable and adhesive, with low stiffness, whereas C4-2 were characterized by moderate deformation, very low stiffness and moderate adhesion (**Figure 12**, control panels). Such diversity of nanomechanical profiles positioned these cultured cell lines as good models representing prostate cancer cells on distinct stages of invasive spread.

As a next step, we co-cultured the model prostate cancer cells for 24 hours with *in vitro* differentiated and polarized model human macrophage-like cells derived from monocytic U937 cell line. All three prostate cancer cell lines were expressing GFP for unequivocal identification of prostate cells in co-culture. We used differentiated, non-polarized M0-like naïve macrophages; M1-like polarized or M2-like polarized U937-derived macrophages in a 1:1 ratio with cancer cells. Single cancer cells were phenotyped with AFM, as in the above-described control experiments, adding 277 cells to the analysis. Apparently, co-culture with all types of model macrophages affected nanomechanical profiles of prostate cancer cells, however extend and direction of changes depended both on the polarization of immune cells and the specifics of cancer cell line (**Figure 12**). To further assist in the analysis of macrophages-induced phenotypic changes, we categorized cells from each of the lines into four classes according to mechanical fitness (**Figure 13**). Control 22Rv1 had approximately equal representation of classes with low to high relative fitness (**Figure 13A**), in DU145 the moderate-fitness class prevailed (**Figure 13B**), whereas majority of tested C4-2 cells were well fit in terms of softness, however moderately prepared for potential cell-cell interactions (**Figure 13C**). The phenotypes of 22Rv1 cells were affected the most by M2-like macrophages, with significantly softer but less adhesive cells after co-culture (**Figures 12A, 13A**). The class 4 of stiff cells disappeared entirely from co-cultures with M2. Co-culture with M0 and M1-like macrophages was accompanied by a moderately increased participation of soft and adhesive cells (**Figure 13A**). Interestingly, co-culture with M1-like macrophages was accompanied by the most pronounced changes in nanomechanical phenotype of DU145: classes of very soft as well as soft and adhesive cells prevailed (**Figures 12B, 13B**). Still, adhesion of tumor cells systematically increased with not only M1 but also M0 and M2 macrophages as partners in co-culture (**Figure 13B**). In turn, the C4-2 cells responded similarly to the presence of all types of macrophages: a sizable fraction of cells retained high softness and attained higher adhesion (**Figures 12C, 13C**). Accordingly, both adhesion and deformability increased significantly after co-culture with M0, M1 and M2-like macrophages (**Figure 12C**). In general, co-culture with polarized macrophages seemed to have

more pronounced influence on nanomechanical phenotypes than co-culture with naïve macrophages (**Figure 14A-C**). Comparison of nanomechanical parameters of patient-isolated CTCs and model cultured cells confirmed that co-culture with model macrophages was always promoting fitness: high adhesion, high deformability and low stiffness, with majority of 22Rv1 and C4-2 cells still remaining within the range of the mechanical similarity to CTCs (**Figure 14D**).

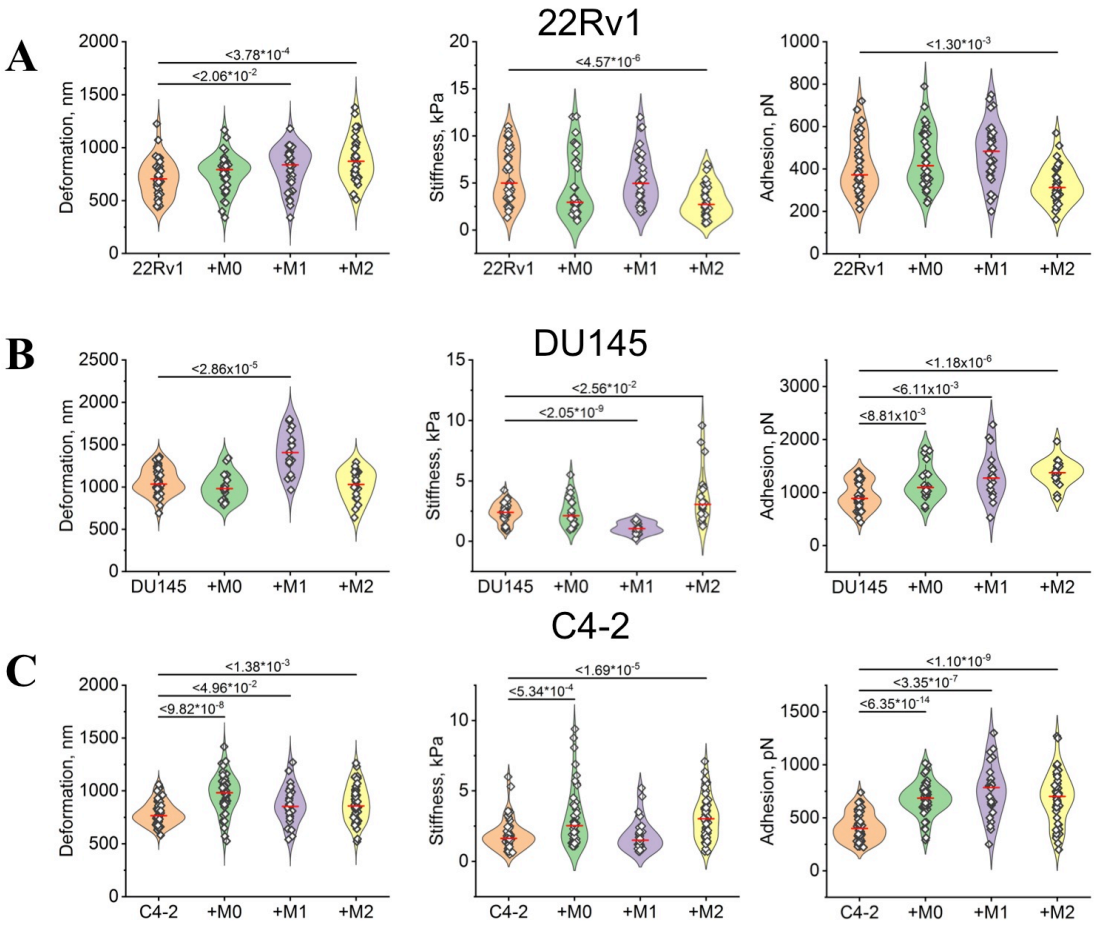

Figure 12 Nanomechanical parameters of human cultured prostate cancer cells specifically respond to co-culture with model macrophages. **A**. Nanomechanical parameters of 22Rv1 cells, control and co-cultured with model macrophages of distinct polarization. **B**. DU145 cells and **D**. C4-2 cells.

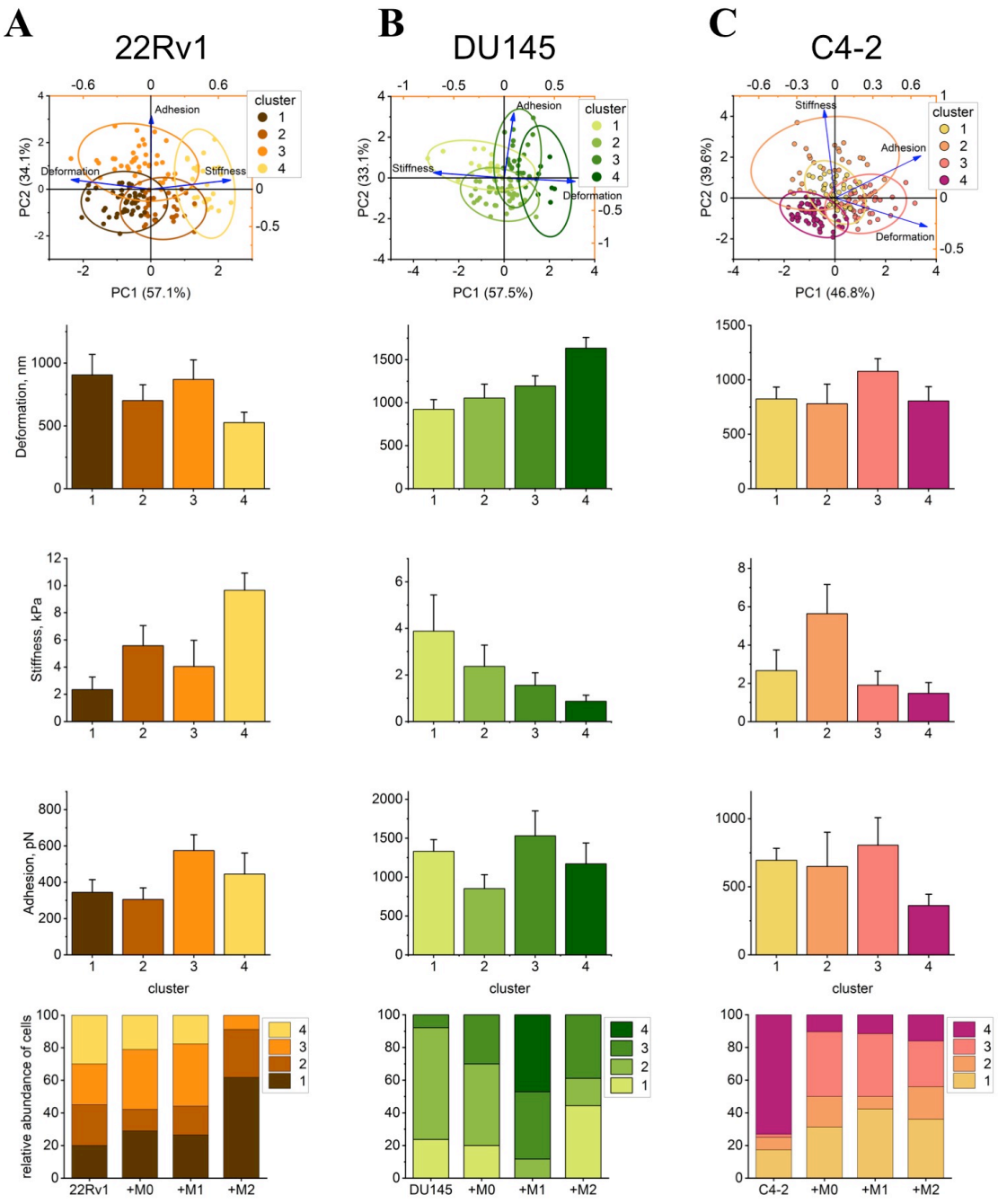

Figure 13 Mechanical phenotypes of cultured cancer cells respond distinctly to co-culture with model macrophages. Increased partition of mechanically well-fitted cells is a common trait of cancer cells exposed to macrophages. In columns from the top: PCA analysis of nanomechanical parameters of single cells, average parameters of cells' classes distinguished by PCA, partition of cells' classes in control and co-cultured preparations. For each cell line the two classes colored in darker shades are considered well mechanically fitted. A. DU145 cells. B. 22Rv1 cells. C. C4-2 cells.

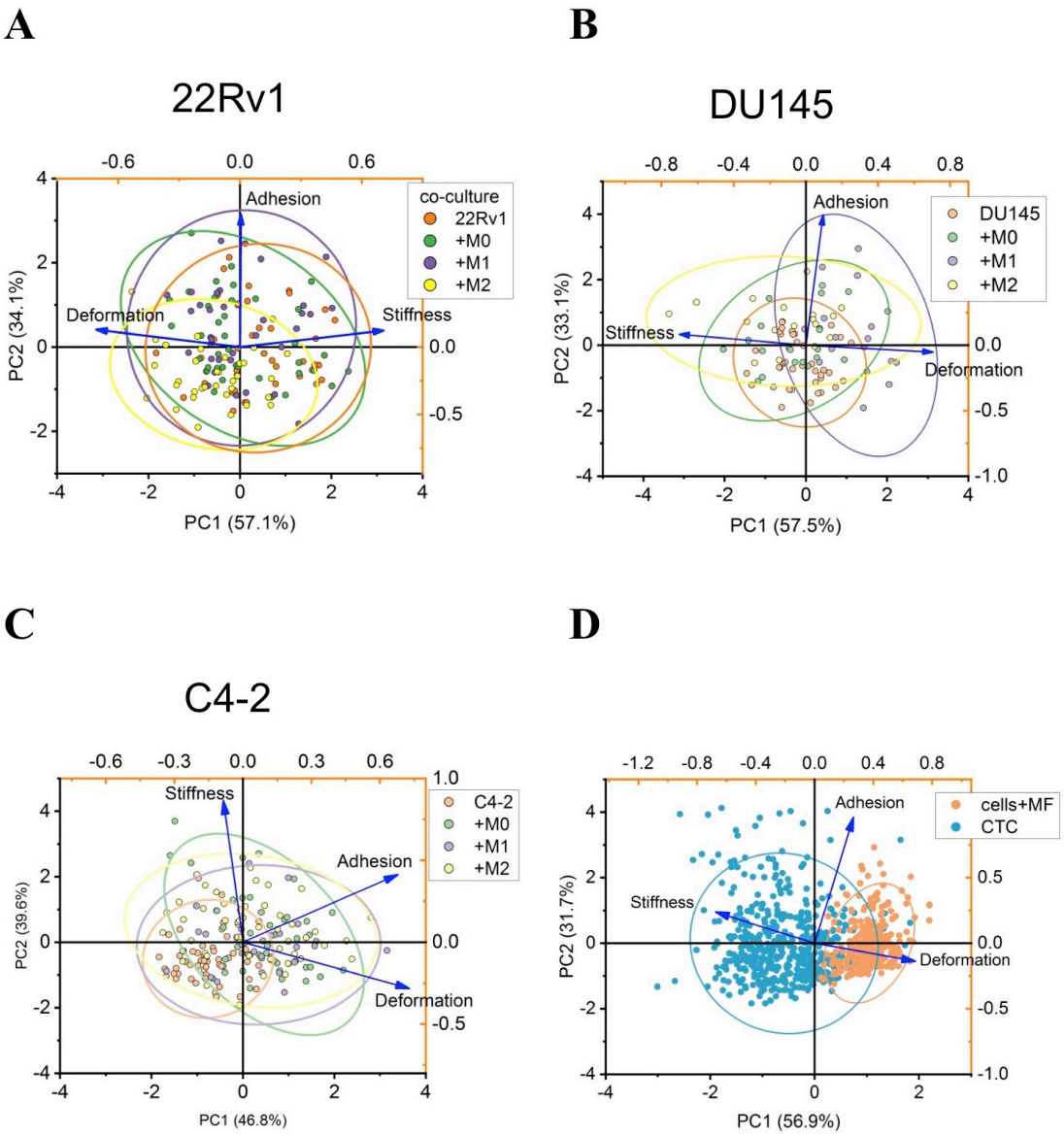

Figure 14 PCA analysis of nanomechanical parameters of single prostate cancer cells, control or co-cultured with model macrophages (U937). Cell lines: **A** - 22Rv1, **B** - DU145, **C** - C4-2. Compare with Figure 11. The presence of macrophages was accompanied by shifts in mechanical phenotypes of all cells. Differentiated, non-polarized M0 macrophages had relatively least influence on the phenotypes their co-culture partners. D. Comparison of patient-isolated CTCs and cultured prostate cancer cells co-cultured with macrophages (M0, M1, M2). Nanomechanical parameters of cultured cells remained within or close to the range parameters determined for CTCs. The out-of-range cultured cells were more adhesive and softer than typical CTCs.

To complete *Subtask 3* within the *Major Task 7* we performed mass cytometry analysis of model prostate cancer cells, control and co-cultured with model macrophages (U937). As declared in the previous report, we choose exceptionally sensitive mass cytometry analysis rather than RNA-based gene expression analysis, to better reflect the actual changes in proteomic profiles of the macrophages – challenged cells.

To track molecular mechanisms behind the changes in nanomechanical phenotype with proteomic analysis we choose DU145 cells. These cells responded to co-culture with macrophages with the most pronounced AFM-detected shifts (**Figures 12-14**). GFP-DU145 cultured alone (control) or with M0, M1 or M2- model macrophages were separated from immune cells in Cytobank and subjected to cytometry by time-of flight (CyTOF) with epithelial/mesenchymal panel of 16 antibodies (**Figure 15**). t-Distributed Stochastic Neighbor Embedding (t-SNE) projections of treatments of DU145 cells are presented in Fig. 7B. Each of four treatment-populations was further divided into subpopulations with distinct proteomic marker profiles for eight mesenchymal and seven epithelial markers (**Figure 15B**). As evident in **Figure 15C**, the cells expressed both epithelial and mesenchymal markers. For example, in control cells high levels of mesenchymal β-catenin, vimentin, N-cadherin and Slug were accompanied by high levels of epithelial EpCAM, cytokeratins (CK) 8/18 and ZO2. This profile remained mixed EMT/epithelial after co-cultures with macrophages: levels of selected epithelial and mesenchymal markers still remained high (**Figure 15C**). However, cumulative analysis revealed that contribution of mesenchymal markers systematically decreased upon co-culture with macrophages, with polarized macrophages triggering stronger shifts than M0-like immune cells (**Figure 15D,E**). These changes mirrored those in nanomechanical phenotype of DU145 cells, where co-culture with M1 and M2 introduced stronger fitness-promoting trends than M0 (**Figure 12**). Apparently, the mechanical fitness beneficial for CTC survival was supported by a partial reversion from an advanced mesenchymal to a more-epithelial phenotype. A striking example of reversion is a decreasing level of TWIST and N-cadherin accompanied by increasing level of E-cadherin in DU145 cells co-cultured with M2 macrophages (**Figure 15C**). In the course of standard EMT TWIST is repressing transcription of E-cadherin. Contribution of oncogenic signal components followed the hybrid EMT/epithelial profile as well: certain markers such as VEGFR1 or Wnt5a were at the highest in control DU145 cells, however some others, most notably SMAD2, EGFR and P-ERK1/2 attained high levels in the co-cultured cells (**Figure 15F**). It seems that cancer cells trained by macrophages may forgo certain features of invasive mesenchymal phenotype in favor of hybrid EMT promoting mechanical endurance especially important for CTCs in circulation. Maintaining the high adhesion and high softness appears to be the most distinctive manifestation of CTC-relevant hybrid EMT.

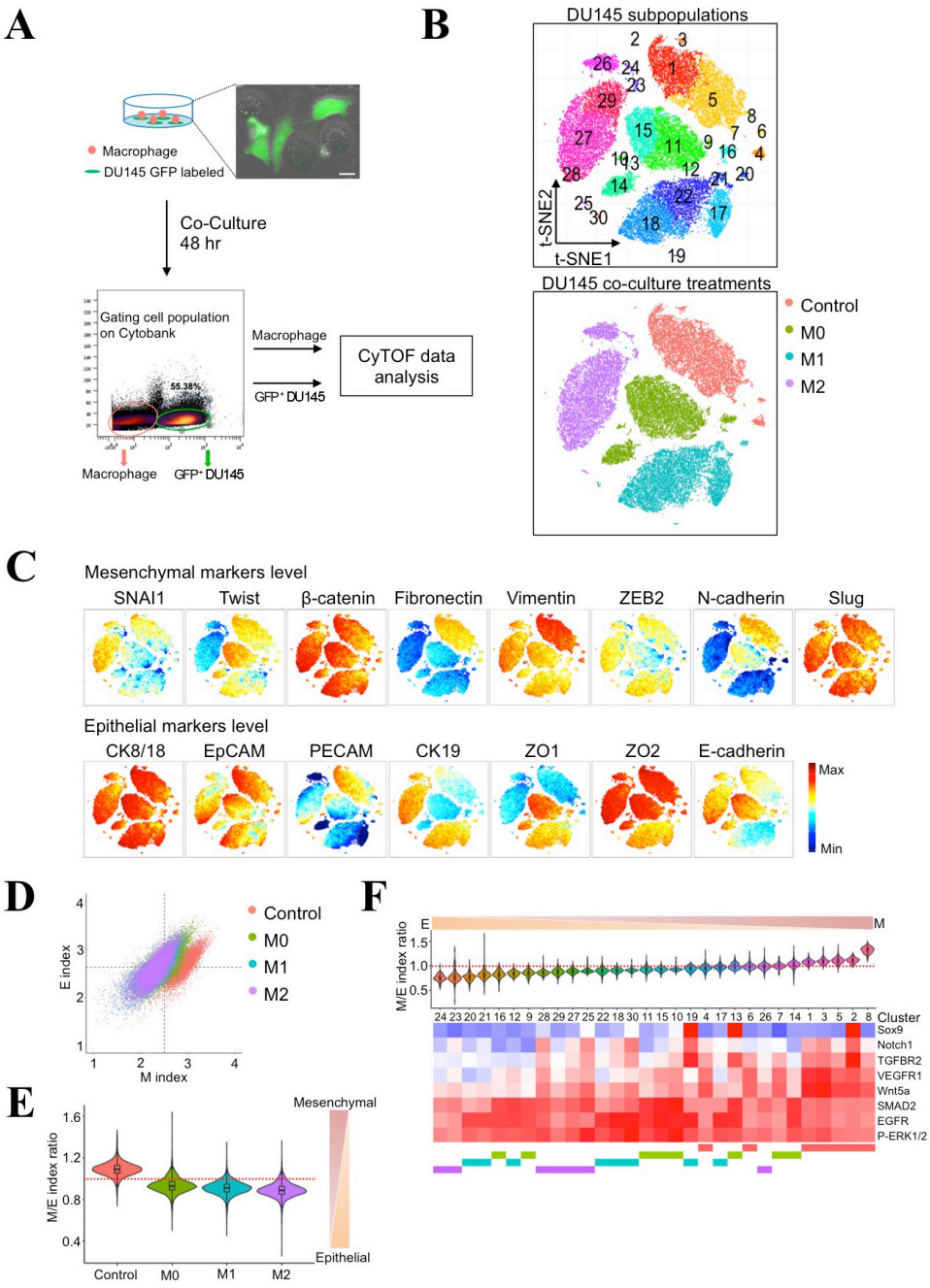

Figure 15 Subpopulations of prostate cancer DU145 cells co-cultured with model macrophages (U937) display hybrid EMT. A. GFP-DU145 were separated from macrophages in Cytobank and subjected to CyTOF analysis with epithelial/mesenchymal panel of 16 antibodies. **B**. t-SNE projections of treatments of DU145 cells. Each of four treatment-populations was further divided into subpopulations. **C**. Profiles of selected epithelial and mesenchymal markers under distinct co-culture conditions. **D**. Scatter plot of Mesenchymal (M) and Epithelial (E) indices amount treatments. **E**. Violin plots of M/E ratio. **F**. Heat map of oncogenic signal components of each cluster aligned based on M/E ratio order.

3.2.8 Specific Aim 3, Major Task 8

To date, samples were collected for 15 patients with both t0 and t1 visits (**Table 1**). Collection of patients' blood samples was postponed for five months due to COVID-19 pandemic, however it resumed since the end of July and *Subtasks 1 and 2* are in progress. Importantly, clinical status: sensitivity or resistance to ADT, of several patients, was recognized even when blood samples for TACCs analysis were not collected. Therefore, during the time of hiatus in new data collection we advanced *Subtask 3* by performing test analyzes with the already available information.

Highly encouraging results of test cluster analysis are presented in **Figure 16**. Mechanical phenotypes and enumerations of TACCs isolated from patients that remained CS tend to cluster together ("red cluster", **Figure 16**). Also, all except one patient (No. 10) in this cluster were non-metastatic. In all other clusters there was a diverse mix of CS and CR as well as non-metastatic and metastatic patients. Interestingly, we noticed trends for metastatic sites: "blue cluster" contained cases with bone metastases (or non-metastatic), whereas the "navy cluster" contained cases with distant lymph nodes spread (or non-metastatic) (**Figure 16**, far left panel).

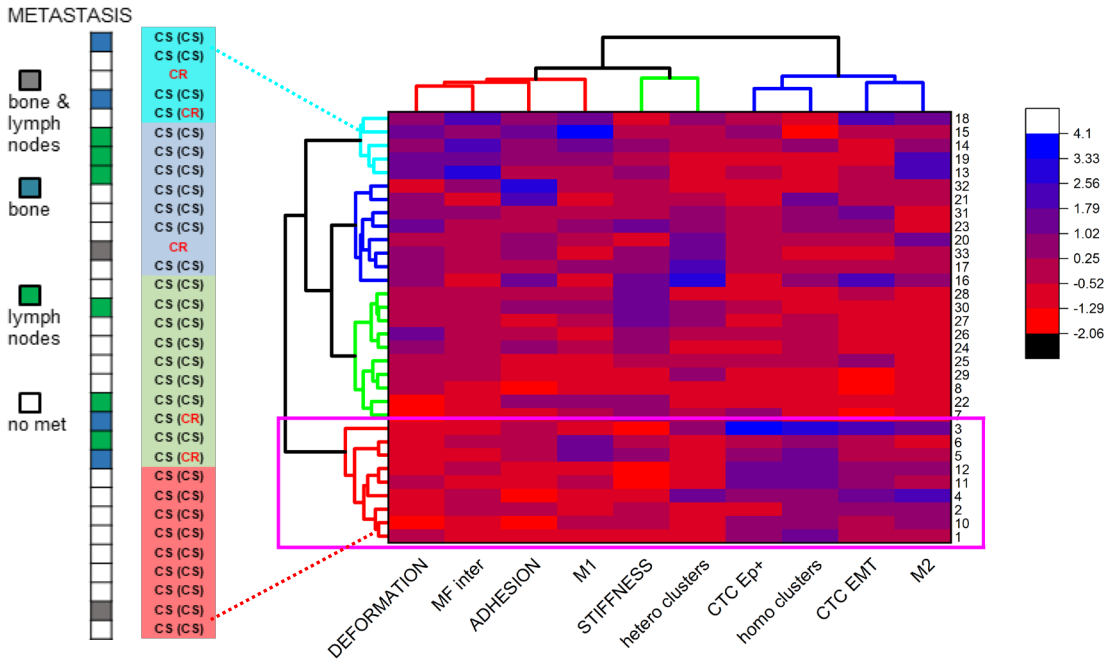

Figure 16 Cluster analysis of mechanical and enumeration parameters of TACCs distinguishes four groups of patients' samples. The pink-framed cluster consists of t0 samples, with a sole exception of sample No. 2. Other clusters have a mixed t0 and t1 representation. In the No. 2 case the pseudo-t0 blood sample was obtained only 3 months after the start of ADT. The panel on the left presents the status of sensitivity to ADT in the clusters. The status in parentheses indicates a clinical update at least 6 months after the blood sample was obtained and the first-time ADT or other therapy was initiated. The far-left strip presents the status of metastasis. Coded identity labels for patients/samples are shown on the right.

Following the trends we inquired if our cluster analysis of mechanical and enumeration parameters would separate cases according to a metastatic spread status. The result is presented in **Figure 17**. Cases with metastatic spread mostly to distant lymph nodes formed a separate cluster, ditto non-metastatic cases. We may speculate that non-metastatic patients that clustered alongside those with distant spread possibly will be diagnosed with metastasis shortly (**Figure 17A**). We will closely follow these cases. As evident in **Figure 17B**, the clustering relied on very specific parameters, for example CTC stiffness for cases with bone metastasis (understandable if a significant portion of CTCs originated in bone) or enumerations of macrophages and EMT CTCs for cases with metastasis to distant lymph nodes. Interestingly, enumeration of intermediate macrophages was of highest relative importance for building the model, followed by enumeration of EMT CTCs and adhesion of CTCs (**Figure 17C**). The potential metastasis-related prospective power may become a bonus feature of our analysis, focused on prediction of castration resistance.

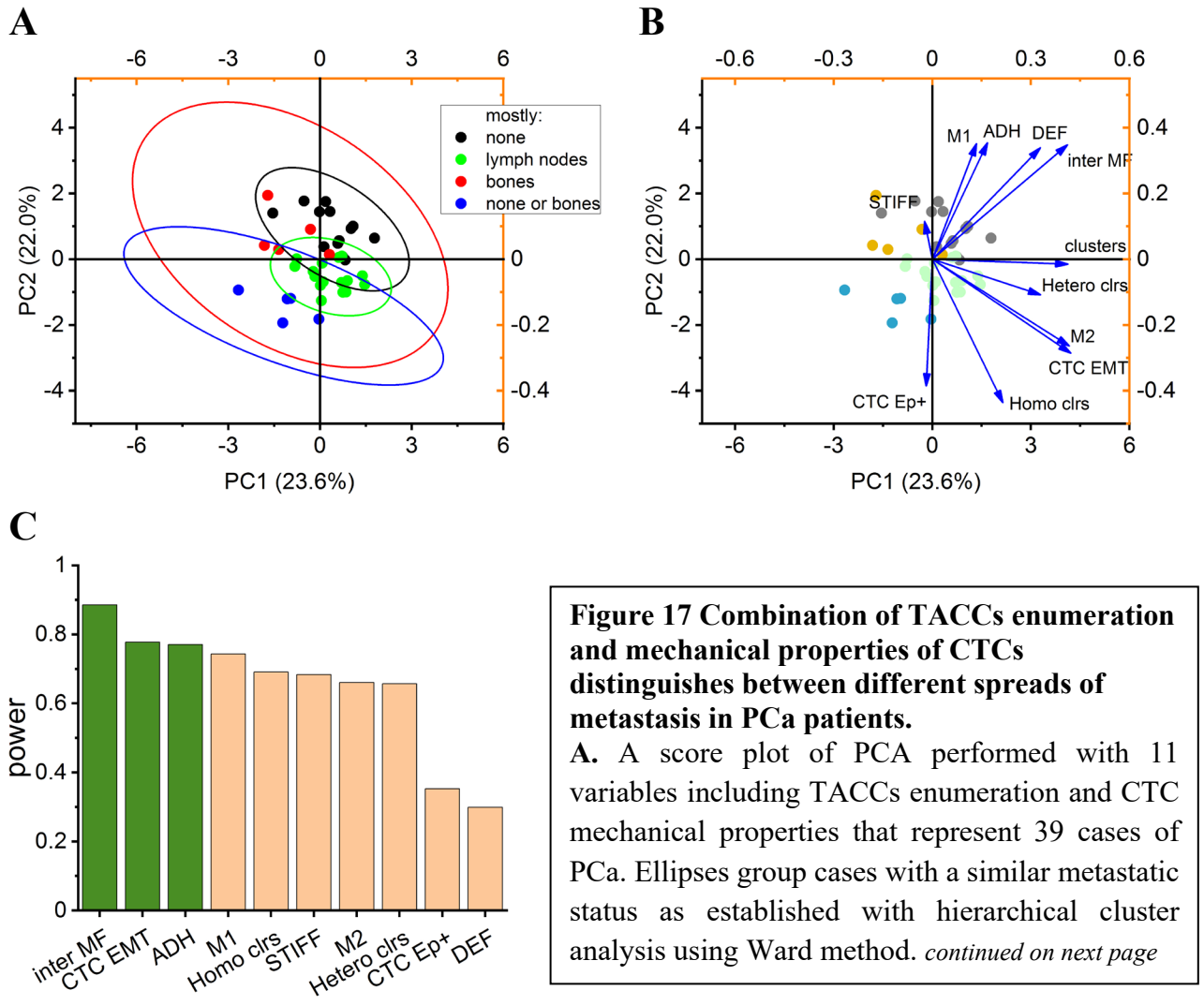

Figure 17 Combination of TACCs enumeration and mechanical properties of CTCs distinguishes between different spreads of metastasis in PCa patients.

A. A score plot of PCA performed with 11 variables including TACCs enumeration and CTC mechanical properties that represent 39 cases of PCa. Ellipses group cases with a similar metastatic status as established with hierarchical cluster analysis using Ward method. *continued on next page*

Figure 17 ***continuation***
Three groups were identified: no distant metastasis, metastasis to lymph nodes, and metastasis to bones. The fourth group ("none or bones") contains almost exclusively cases with the previous surgery treatment but distinct metastatic outcomes. Each group contains certain number of cases with undetected metastasis suggesting a possible trajectory of diseases progression.
B. A loading plot of PCA presented in figure A. Th e first four principal components explain about 71.7% of the variable variance. The cluster labeled as without detected metastasis is distinguished by a high enumeration of M1 and intermediate MFs, and high CTCs adhesion and deformation. The cluster of cases with metastasis to bones shows higher CTCs stiffness. The cluster of cases with metastasis to lymph nodes has a higher enumeration of CTCs classified as EMT, M2 MFs, and homo clusters. Finally, the diverse cluster of "no metastasis or to bones" cases exhibits a high enumeration of EpCAM positive CTCs in combination with low CTCs adhesion.
C. A column graph presenting the relative importance of variables selected for PCA. The larger power indicates a higher relevance for building the PCA model. The highest relevance was detected for intermediate MFs, enumeration of EMT CTCs and average adhesion of CTCs. They are closely followed by enumeration of M1 MFs and homo clusters, and CTCs stiffness.

The predictive potential of TACCs phenotyping may be understandably limited to a time of several months. For example, in the case of patient No. 7 (t0) - 8 (t1) the phenotyping indicated rather poorly fit CTCs during first (No. 7; t0) and second (No. 8; t1) visits, correctly predicting castration sensitivity (**Figure 4**). However, more than a year later, after additional treatments and another round of ADT the patient was diagnosed with castration resistance. We may speculate that a relatively large advance of mechanical phenotype toward higher fitness between t0 and t1 in this case (**Figure 4**) indicated the future failure of therapy – a notion worth to explore.

3.3 Opportunities for training and professional development provided by the project:

- Dr. Chia-Nung Hung, Postdoctoral Fellow, is continuing his work on single-cell molecular analysis of TACCs. In addition to gene expression analysis he mastered mass cytometry proteomic profiling of cells and generated data for *Major Tasks 4* and *7*. He is a co-author of the submitted manuscript.

- Yusheng Qian, M.Sc., a PhD Graduate Student in Molecular Medicine is continuing his work on the project. Mr. Qian is mentored by Drs. Gaczynska and Osmulski and most recently he was admitted to PhD candidacy. He generated data for *Major Tasks 5 and 7,* and the project will constitute a core of his PhD thesis. He is a co-author of the submitted manuscript. He mastered a unique method of AFM-based characterization of single cell-

cell interactions and is currently preparing a first-author manuscript describing the use of the method in the cell culture model of EMT.

3.4 Dissemination of the results to communities of interest:

- Seminar presentation "From molecules to cells: the power of atomic force microscopy.", Department of Biochemistry and Structural Biology, UT Health SA, September 2019. Presenters: Drs. Gaczynska and Osmulski. The presentation was listed as planned in the previous Report.

  COMMENT: Nearly all plans for dissemination in this reporting period were unfortunately destroyed by pandemic measures. National and local scientific meetings were either cancelled or moved to late fall or next calendar year. For the nearest future we are planning two poster presentations on the virtual Biophysical Society Meeting in February 2021, with the graduate student Yusheng Qian and Dr. Osmulski as presenters.

3.5 Plans for the next reporting period:

We will continue the study following the Statement of Work for months 24-36.

- A final cohort of patients should be accrued.
- Mechanical and immunochemical profiles will be collected for all accrued patients.
- All collected biophysical and molecular data will be analyzed.
- Statistical analysis of mechanical, immunochemical, molecular and clinical data will be performed.
- Model cell culture experiments involving cultures challenged with fluid shear stress (FSS; "model circulation") will be finished. The data will be integrated with those obtained for already completed stationary cultures experiments for an integrated model of CTCs behavior.

4. Impact

4.1 Impact on the development of the principal discipline of the

project. The major findings in this reporting period are outlined below.

- We confirmed and refined our initial finding that patient isolated CTCs and model prostate cancer cells display a hybrid epithelial-mesenchymal features. High adhesiveness (epithelial trait) emerges as the major nanomechanical parameter distinguishing aggressive tumor cells from aggressive CTCs. The most aggressive tumor cells switch from epithelial-like to mesenchymal-like phenotype, with lowered adhesiveness and increased motility (invasiveness). However, the most invasive circulating tumor cells retain high adhesion as a survival measure and special adaptation to mechanical stress endured in the bloodstream environment. Based on our cultured cells and CTCs data, we

hypothesize that invasive tumor-residing cells already advanced on the EMT axis may reverse to regain high adhesion, useful for survival-promoting clustering in circulation.
Significance: the finding broadens the knowledge about the diversity of epithelial-to-mesenchymal transition processes that occur during normal development and differentiation but also accompanies cancerous spread. Our idea of reverse-EMT is novel and we will pursue this trait vigorously. The knowledge will impact development of anti-metastasis therapies, with targeting adhesiveness of CTCs as a worthy goal not explored before.

- Our initial observations based on a limited number of patients suggest that whereas high adhesiveness of CTCs is hallmark of poor prognosis in low disease burden patients, in patients with a rapidly advancing disease the adhesion of CTCs decreases, apparently for massive metastatic spread. Low adhesion is established marker of advanced EMT, confirmed in our model cell culture studies. The seemingly conflicting marker measures are reliably distinguishable when the profile of patient's circulating macrophage population is taken into account. We will vigorously pursue this observation.
  Significance: the finding broadens the knowledge about the diversity of EMT in CTC population and points at important prognostic and predictive biomarker measures.

- Correlative studies link mechanical fitness of patient-isolated CTCs with abundance of macrophages with markers of TAMs. We speculate that macrophages that co-purify with CTCs are in fact TAMs that escaped the tumor, possibly in clusters with CTC.
  Significance: Enumeration of macrophages emerges as a predictive marker, alone or together with mechanical phenotype and enumeration of CTCs. Targeting macrophages emerges as a viable anti-metastatic strategy.

- We confirmed that model macrophages promote "mechanically fit" phenotype in cultured cancer cells in a stationary co-culture model. Adhesion of model CTCs is the mechanical parameter most profoundly affected (an increase) by the presence of macrophages. The standard stationary co-culture may be considered a model for conditions in the tumor periphery, where "future CTCs" reside before escaping the tumor. We hypothesize that "future CTCs" are trained by TAMs to attain mechanical fitness. We found that macrophages of diverse polarizations, not only anti-inflammatory, can promote the fitness, in a full agreement with our data on patient-isolated TACCs. Importantly, the
  Significance: targeting macrophages emerges be a viable anti-metastatic strategy.

4.2 Impact on other disciplines.
Nothing to Report

4.3 Impact on technology transfer.
Nothing to Report

4.4 Impact on society beyond science and technology. *Nothing to Report*

5. Changes/problems

5.1 Changes in approach and reasons for change.

There are no significant changes in approach. Minor changes and additions:

- As declared in the previous Report, we added protein transcription profiling by flow cytometry/mass spectrometry CyTOF system to our analysis of cultured cells (*Major Tasks 5 and 7*). This extremely effective technology available in the UT Health BioAnalysis and Single Cell Core (BASiC) increases the volume of information collected and available for the final model construction. The proteomic profiling replaced gene expression profiling.

- In the previous Report we presented data on the profound effects of fluid shear stress (FSS; "model circulation") on the molecular and mechanical phenotypes of model CTCs. We continue these very informative experiments to supplement *Major Tasks 5 and 7* beyond the already finished declared works.

5.2 Actual or anticipated problems or delays.

The COVID-19 pandemic caused a five-month break in new patients' accrual and a slowdown in collection of t1 samples. Importantly, we still obtained critical clinical information about the already enlisted patients. Normal pace of accrual and sample collection resumed at the end of July. We anticipate an about five month delay in accrual of the planned number of patients and collection of full set of samples.
Also, the pandemic hampered data presentation to scientific community - see **3.4** Dissemination of the results to communities of interest).
.

5.3 Changes that had a significant impact on expenditures.
None

5.4 Significant changes in use or care of human subjects/vertebrate animals/biohazards/select agents.
None

- **6. Products**
- *Manuscript submitted (Cancer Research):*

Pawel A. Osmulski, Alessandra Cunsolo, Meizhen Chen, Yusheng Qian, Chun-Lin Lin, Chia-Nung Hung, Devalingam Mahalingam, Nameer Kirma, Chun-Liang Chen, Josephine A. Taverna, Michael Liss, Ian M. Thompson, Tim H.-M. Huang, and Maria E. Gaczynska "Aggressive nanomechanical phenotype of circulating tumor cells in prostate cancer is promoted by contacts with macrophages."
-

7. Participants

7.1 Individuals working on the project

Name	Tim H. Huang
Project Role	PI
Researcher Identifier (e.g. ORCID ID):	0000-0001-5985-9176
Nearest person month worked:	0.96 cal. mo.
Contribution to Project:	Oversight and coordination of the project
Funding Support:	No Change

Name	Maria Gaczynska
Project Role	Co-Investigator
Researcher Identifier (e.g. ORCID ID):	0000-0002-9033-5706
Nearest person month worked:	3 cal. mo.
Contribution to Project:	Collection and analysis of immunofluorescence images of TACCs, design and oversight of co-culture experiments.
Funding Support:	No Change

Name	Pawel A.Osmulski
Project Role	Co-Investigator
Researcher Identifier (e.g. ORCID ID):	0000-0002-5359-9200
Nearest person month worked:	1.8 cal. mo.
Contribution to Project:	Collection and analysis of mechanical phenotypes of patient isolated and model CTCs, design of co-culture experiments.
Funding Support:	No Change

Name	Chun-Liang Chen
Project Role	Co-Investigator
Researcher Identifier (e.g. ORCID ID):	0000-0002-6774-9003
Nearest person month worked:	1.2 cal. mo.
Contribution to Project:	Collection of cells for single-cell gene expression analysis, single cell gene expression analysis of selected CTCs.
Funding Support:	No Change

Name	Michael Liss

Project Role	Co-Investigator
Researcher Identifier (e.g. ORCID ID):	0000-0001-6978-1026
Nearest person month worked:	.36 cal. mo.
Contribution to Project:	Coordination of patients' accrual, collection of clinical data.
Funding Support:	No Change

Name	Byeongyeob Choi
Project Role	Co-Investigator
Researcher Identifier (e.g. ORCID ID):	
Nearest person month worked:	.6 cal. mo.
Contribution to Project:	Processing of data for statistical analysis
Funding Support:	No Change

Name	Meizhen Chen
Project Role	Research Scientist
Researcher Identifier (e.g. ORCID ID):	
Nearest person month worked:	.6 cal. mo.
Contribution to Project:	Co-culture experiments with model CTCs and macrophages.
Funding Support:	No Change

Name	Chia-Nung Hung
Project Role	Research Scientist
Researcher Identifier (e.g. ORCID ID):	
Nearest person month worked:	3 cal. mo.
Contribution to Project:	CyTOF analysis of model CTCs and macrophages, collection of cells for single-cell gene expression analysis, single cell gene expression analysis of selected CTCs, model CTCs and model macrophages.
Funding Support:	No Change

Name	Yusheng Qian
Project Role	Graduate Student
Researcher Identifier (e.g. ORCID ID):	
Nearest person month worked:	6 cal. mo.

Contribution to Project:	Co-culture experiments with model CTCs and macrophages, collection and analysis of mechanical phenotypes of model CTCs.
Funding Support:	No Change

7.2 Changes in the active other support of PD/PI and key personnel
Nothing to report

7.3 Other organizations involved as partners
Nothing to report

8. Special Reporting Requirements
Nothing to report

9. Appendices

Aggressive Nanomechanical Phenotype of Circulating Tumor Cells in Prostate Cancer is Promoted by Contacts with Macrophages.

Pawel A. Osmulski[1]*, Alessandra Cunsolo[1], Meizhen Chen[1], Yusheng Qian[1], Chun-Lin Lin[1], Chia-Nung Hung[1], Devalingam Mahalingam[2, 3], Nameer Kirma[1], Chun-Liang Chen[1], Josephine A. Taverna[3], Michael Liss[4], Ian M. Thompson[4, 5], Tim H.-M. Huang[1], and Maria E. Gaczynska[1]*

[1]Department of Molecular Medicine, University of Texas Health Science Center at San Antonio, San Antonio, Texas, USA

[2]Department of Hematology and Oncology, University of Texas Health Science Center at San Antonio/Mays Cancer Center, San Antonio, Texas

[3]Current address: Robert H Lurie Medical Research Center, Northwestern University, Feinberg School of Medicine, Chicago, Illinois

[4]Department of Urology, University of Texas Health Science Center/Mays Cancer Center San Antonio, Texas, USA

[5]Current address: CHRISTUS Santa Rosa Hospital - Medical Center, San Antonio, Texas

Running Title:

Macrophages Promote Aggressive Mechanical Phenotype of CTCs.

Keywords:

Circulating tumor cells, macrophages, prostate cancer, atomic force microscopy, metastasis.

Additional information:

*corresponding authors:

Maria Gaczynska, Ph.D.

Department of Molecular Medicine, University of Texas Health at San Antonio,

15355 Lambda Drive, San Antonio, 78245 TX, USA; phone: (210) 567-7262

Gaczynska@uthscsa.edu

Pawel A. Osmulski, Ph.D.

Department of Molecular Medicine, University of Texas Health at San Antonio,

15355 Lambda Drive, San Antonio, 78245 TX, USA; phone: (210) 567-7262

Osmulski@uthscsa.edu,

Conflict of Interest: The authors declare no potential conflicts of interest.

Manuscript information: word count, number of figures and tables,

Abstract

Aggressive tumors of epithelial origin shed cells that intravasate, become blood borne as circulating tumor cells (CTCs), and die or start metastases. We demonstrated before that CTCs isolated from the blood of prostate cancer patients display specific nanomechanical phenotypes indicative of the cells' endurance and invasiveness and the patients' sensitivity to androgen deprivation therapy. Here we report that patient-isolated CTCs are nanomechanically distinct from cells randomly shed from tumor, with high adhesion as the most striking biophysical marker. Moreover, CTCs uniquely co-isolate with macrophage-like cells bearing the markers of tumor-associated macrophages (TAMs). Prominent presence of these immune cells was indicative of survival-promoting phenotype of "mechanical fitness" in CTCs: high softness and high adhesion determined by atomic force microscopy (AFM). Correlations between enumeration of macrophages and mechanical fitness of CTCs were especially strong in patients before the start of hormonal therapy. In a search for mechanisms determining mechanical fitness of cancer cells we attempted to recapitulate the tumor cells - macrophages contacts in cell culture. Single-cell proteomic analysis and nanomechanical phenotyping revealed that immune cells promoted hybrid EMT (epithelial-mesenchymal transition) manifesting in mechanical fitness. We postulate that selected tumor cells are coached by TAMs and accompanied by them to acquire hybrid EMT. The resulting well-mechanically fit CTCs survive the critical early stage of circulation thanks to softness bestowing resistance to shear stress, and adhesiveness enabling protective cell clustering.

Introduction

Circulating tumor cells (CTCs) are shed by aggressive epithelial-origin tumors and are found in the bloodstream of patients at the risk of metastasis or with already detected metastatic growth (1). CTCs are as rare as one in a billion of blood cells, however due to their unique properties such as large size and epithelial surface markers they can be isolated by microfiltration or immunoaffinity capture from a “liquid biopsy”: few milliliters of a patient’s peripheral blood (2). Since the bloodstream is not a natural environment for epithelial-like CTCs, majority of them die by mechanical stress, apoptosis or anoikis, or due to attacks from immune cells (3). The surviving few CTCs progress with epithelial-to-mesenchymal transition (EMT), extravasate and start new tumor growth in distant tissues (2). Enumeration of CTCs is used as a general prognostic biomarker, with serious attempts to a more advanced precision medicine related analysis (4). Indeed, the enumeration-only approach centered on EpCAM (epithelial cell adhesion molecule) positive cells neglects cells with advanced EMT and may miss the opportunity to determine metastatic potential among heterogeneous CTCs (5,6). Since successful CTCs need a specific set of adaptations to withstand conditions in the bloodstream, we turned our attention to their physical endurance. Mechanical challenges during intravasation, circulation, and extravasation point at the physical properties of CTCs as crucial factors influencing the cells’ capability to survive the hostile environment (7). These physical properties are tightly connected with EMT that involves a massive remodeling of the cytoskeleton and membranes (8) affecting cell softness and adhesion. CTCs express a wide spectrum of both epithelial and mesenchymal marker proteins and EMT traits are considered biomarkers of poor prognosis (9,10). However, recent evidence indicates that aggressive CTCs may undergo a partial/hybrid EMT to preserve or promote features supporting their survival in the bloodstream (9,11,12). For example, plakoglobin implicated in survival-promoting CTC clustering is a component of epithelial, not mesenchymal cell junctions (13), The mechanism and extent of hybrid EMT (or epithelial/mesenchymal plasticity) in tumor cells and CTCs as well as its clinical significance in metastatic potential remains controversial (14,15).

In our previous works, we have demonstrated that CTCs isolated from the blood of castration resistant patients are significantly less stiff, more deformable and more adhesive than CTCs from castration sensitive patients with less aggressive disease responding to androgen deprivation therapy (ADT) and at low risk of fast metastatic spread (16). We described these distinctive mechanical properties of CTCs isolated from castration resistant patients as cell survival and resilience promoting “mechanical fitness”: a particular combination of low stiffness, high deformability and high adhesion. We envision that such CTCs not only escape death but also may invade distant tissues. To measure the properties of fitness, we applied mechanical profiling of

cells with the super-sensitive Peak Force Quantitative Nanomechanical mode of atomic force microscopy (PF-QNM AFM). In this method, a micro-probe scans the surface of a live cell by indenting it with a nano-scaled force (Fig. 1A). Physical parameters of the probe's interactions with the cell during the single non-destructive, few-minutes scan are recorded and translated into maps of nanomechanical parameters: stiffness, deformability and adhesion (Fig. 1A, B). Stiffness, the most often used nanomechanical parameter, describes how much pressure is needed to indent the cell in a reversible (elastic) manner. Stiffness is presented as the object-inherent Young modulus in units of pressure (Pascals; Pa). High Young modulus is manifested as high stiffness and low elasticity (Fig. 1A). Stiffness of live cells may range two orders of magnitude from a fraction of kPa to over 10 kPa, however cancer cells are generally less stiff (more elastic) than their non-cancerous counterparts (17,18). The depth of indentation enforced by the probe with a preset force and without cell fracturing is a measure of deformability (length unit: nanometers) that includes elastic and non-elastic components (Fig. 1A). Both stiffness and deformability are crucial when cells are subjected to mechanical challenges during intra- and extravasation (16,19,20). We refer to low stiffness accompanied by high deformability as "softness" contributing to mechanical fitness of CTCs. The adhesion (force unit: Newtons) is a measure of force needed to lift the tip from the cell surface during the probe withdrawal (Fig. 1A). Adhesion of mesenchymal cells is typically much lower than epithelial cells, as expected for mobile cells in contrast to sedentary ones (21,22). Interestingly, adhesion of CTCs tends to be relatively high, a hybrid EMT trait important for cell-cell interactions (12,16,22). We use the "high" and "low" designations for parameters in a relative manner, comparing to median values or control, or special conditions, as specified. In a search for mechanisms distancing biophysical features of CTCs from the primary tumor cells we turned our attention to cells accompanying CTCs in the bloodstream. It has been reported that CTCs engage in crosstalk with the blood environment (23) and interact with platelets (24), myeloid derived suppressor cells (25) or neutrophils (26). In addition, a presence of macrophage-like cells have been noted in the blood of patients or model animals with aggressive tumors (22,27). We set to explore links between mechanical fitness of CTCs, the presence of accompanying cells and the clinical status of prostate cancer patients.

Materials and Methods

Human Subjects

Liquid biopsy samples were obtained from male patients following the IRB protocols at the University of Texas Health San Antonio and the Audie L. Murphy Memorial VA Hospital in San Antonio, TX (IRB#HSC20130219H, CTRC#13-0001). Void early morning urine was collected in urine cup (Starplex Scientific) and blood was collected in EDTA-coated tubes (Becton, Dickinson

and Co.) for subsequent analysis. Informed consent was obtained from all subjects. Detailed clinicopathological information on individual patients is provided in Table 1 and Supplementary Table S1. Morphometric data on blood isolated CTCs and immune cells were collected from images obtained for patients described in Osmulski et al. (16).

Isolation, morphometric characterization and enumeration of cells from liquid biopsies.

To recover exfoliated cellular components void urine was centrifuged at 700 g for 5 min, and the supernatant was removed. The pellet was washed with 1 mL of cold PBS and recollected by centrifugation twice. After immunocytochemical staining with specific anti-EpCAM-FITC (StemCell Technologies, clone VU-1D9, Cat#10109) and anti-CD45-PE (Miltenyi Biotech, Cat#130-080-201) antibodies the cells' suspension was captured on glass slides coated with 0.1% polyethylenimine (PEI; Sigma-Aldrich) for nanomechanical phenotyping. The prostate origin of the urine-isolated $EpCAM^+$ cells was confirmed with positive staining for prostate-specific markers PSA and PSMA (anti-PSA: Dako, followed by anti-rabbit Ig-G-Cy3; anti-PSMA: FOLH1-APC, R&D Systems).

TACCs were isolated from patients' blood by size exclusion/microfiltration as previously described (16), using ScreenCell® CC filtration kits (ScreenCell, Westford, MA). Cells captured on the filters were stained with specific anti-EpCAM-FITC (as above) or alternatively anti-vimentin-Alexa 488 (BD Pharmingen, clone RV202, Cat#562338), anti-CD163-PE (BD Pharmingen, clone GHI/61, Cat#560933) and anti-CD80-Cy5 (BD Pharmingen, Cat#559370).

Immunocytochemical staining was carried out by 30 min incubation of cells at room temperature with antibodies diluted 100x in 100 µl of PBS with 2% BSA, followed by 3x washing with PBS.

Morphometric parameters (footprint) of cells were collected from optical images recorded with Nikon Ti inverted epifluorescent microscope, using ImageJ software. Enumeration of TACCs was carried out on optical and fluorescent images recorded with Evos microscope. Enumeration of cells in 7.5 ml of blood is provided.

Cell culture: prostate cancer cells.

Human prostate cancer cell lines DU145, 22Rv1 and C4-2 (derivative of LNCaP) were obtained from American Type Culture Collection (ATCC, Manassas, VA) and cultured in RPMI-1640 medium supplemented with 10% fetal bovine serum and 100 U/mL penicillin/streptomycin. The authenticity of cell lines was confirmed by the STR Testing Service of the ATCC. Nanomechanical profiling was performed on single cells from passages 2 – 4, with cells growing to less than 50% confluence. To assure unequivocal identification of cancer cells in co-cultures, we constructed GFP (green fluorescent protein) – expressing cells for all three lines using lentivirus production system. A shRNA construct for GFP expression had been published before (28). This shRNA-expressing

lentiviral plasmid was cotransfected with plasmids pMD2.G and psPAX2 into 293T cells. Virus-containing medium was collected at 48 h and 72 h after transfection and filtered. For viral transduction into C4-2, 22RV1 and DU145 cells, lentivirus-containing medium was added to each culture at a multiplicity of infection (moi) of 10. Virus-containing medium was removed from cultures 24 h after infection and cells were further incubated for 48 h to ensure GFP expression. The GFP-positive infected cells were sorted by FACS, cultured and cryopreserved. Cells from all three lines stably expressed GFP in the course of all experiments. Nanomechanical parameters of GFP-expressing cell lines were undistinguishable from parent cell lines (data not shown).

Cell culture: model macrophages.

U937 cells were maintained in RPMI-1640 medium supplemented with 10% of heat inactivated fetal bovine serum. U937 Cells were differentiated into macrophages by treatment with PMA (Phorbol 12-myristate 13-acetate) at 100ng/ml for 48hours. PMA was removed, cells were washed and rested in fresh medium for 24 hours. All cells were sedentary, indicating their differentiation. After the resting time, the naïve macrophages were used for co-cultures or polarized. Polarization to M1 was carried out by incubation with LPS (10ng/ml) and IFN-γ for 72 hours, whereas polarization to M2 was attained by incubation with IL-4 (20ng/ml) for 72 hours (29). Status of polarization was confirmed by staining of a cell sample with specific fluoro-labeled antibodies: anti-CD80 and anti-CD163, as described above for patient-isolated CTCs. The model macrophages were used for further experiments when at least 80% of cells in tested sample were $CD80^{+}CD163^{-}$ (M1) or $CD80^{-}CD163^{+}$ (M2). Cells were lifted with non-enzymatic solution (Gibco), counted and added to cancer cells.

Nanomechanical profiling with Atomic Force Microscopy (AFM)

CTCs captured on isolation filters, UPCs immobilized on PEI-coated slides and cultured cells surface-growing on dishes were scanned with a Catalyst Atomic Force Microscope (Bruker) mounted on a Nikon Ti inverted epifluorescent microscope. Nanomechanical parameters of cells were collected in the Quantitative Nanomechanical Mapping (PF-QNM) mode of the AFM. Before AFM imaging, optical images were recorded for each cell. SCANASYST-AIR (Bruker) probes were used for imaging after their spring constant was determined with the thermal tuning. Cell boundaries were located with peak force error (PFE) AFM images and further verified with height images. Nanomechanical parameters of cells were captured in three separate PF-QNM channels: elasticity (Young's modulus), deformation and adhesion. Analysis of these parameters was performed with NanoScope Analysis software v.1.7 (Bruker) using the retrace images (30). Force curves were fit to the Sneddon model, which additionally included adhesion forces and followed the rules proposed

by Sokolov (31,32). Mode values of the mechanical parameters for individual cells were calculated from the corresponding distribution histograms.

Proteomic analysis with CyTOF

After macrophage polarization, C4-2, or 22RV1, or DU145 cells were co-cultured with same number of M1 or M2 macrophages in co-culturing system. C4-2, or 22RV1, or DU145 cells were co-cultured with macrophages for 72 hours. Then, co-cultured cells were harvested for single cells with trypsin and processed for Cytometry by time-of-flight (CyTOF) running. CyTOF Antibodies were conjugated in-house according to the manufacturer's instructions or purchased in pre-conjugated forms from the supplier (Fluidigm; Supplementary Table S3). Briefly, for cell processing cells were harvested and stained with cisplatin and metal-conjugated surface antibodies sequentially for viability and surface staining. After fixation and permeabilization, cells were stained with metal-conjugated antibodies. The cells were then labeled with an iridium-containing DNA intercalator (191Ir+ or 193Ir+) for identification of cell events before analysis on a Helios mass cytometer. Signals were bead-normalized using EQ Four Element Calibration Beads. Signals of samples were normalized using CyTOF software (Version 6.7.1014, Fluidigm). The generated files underwent signal cleanup and filtering for single cells using Cytobank (https://www.cytobank.org/). The gated Flow Cytometry Standard (FCS) files were downloaded for further analysis using Cytofkit. The PhenoGraph clustering algorithm in Cytofkit was implemented in R from the Bioconductor website (https://bioconductor.org/packages/cytofkit/). CyTOF data were clustered and visualized using t-distributed stochastic neighbor embedding (tSNE) algorithm based on normalized expression levels (Z-score) of markers (of protein expression with phenotypically related cells clustered together.

Statistical Analysis

Hierarchical cluster analysis with corresponding heat maps and principle component analysis of the mechanical properties of the cells, and cell enumeration was performed using OriginPro 2020 software (OriginLab) with additional assistance from Statistica (TIBCO). Binary logistic regression was applied to predict odds of cases (OriginLab). Group tests of cell viability among circulating tumor cells were based on Student's t-test. General descriptive statistics was completed with OriginPro.

RESULTS

Tumor-shed cells in blood and urine display distinct nanomechanical phenotypes and co-isolate with distinct populations of immune cells.

In the case of prostate tumors, cancer cells are shed into the blood as CTCs and also to urine as “urine prostate cells” (UPCs) with a biomarker potential (33). Both CTCs and UPCs are exposed to damaging fluid shear stress; however only CTCs may act as “seeds of metastasis” while UPCs inevitably perish. We decided to compare nanomechanical phenotypes of the two classes of cells released from tumor.

Microfiltration of blood collected from patients with aggressive prostate cancer retained cells that permeate through 6.5 micrometer pores. Red and white blood cells, even those of larger diameters, were sufficiently deformable to pass and were not present on filters, as in our previous studies using the microfiltration method (16). Large cells of epithelial-like morphology mostly positive for epithelial marker EpCAM were retained. Large $EpCAM^+$ cells were also abundant in urine sediment collected from prostate cancer patients. AFM analysis was performed on 122 CTCs and 104 UPCs positive for prostate-specific markers PSA/PSMA which were isolated from peripheral blood (n=10) and urine samples (n=11) from individual prostate cancer patients, respectively (Table 1, Supplementary Table S1, Fig. 1B). The patient cohort was comprised of high-risk patients with local disease and patients with low-volume metastatic spread (Table 1, Supplementary Table S1). When principle component analysis (PCA) was used to stratify different biophysical features of these cells, we observed that cell adhesion showed the most striking difference among these exfoliated cells. CTCs appeared five-fold more adhesive than UPCs (594 picoNewtons *versus* 107 pN) (Fig. 1B). Analysis of stiffness and deformability revealed a remarkable diversity among urine-shed cells. Interestingly, we found two very distinct classes of UPCs: one was ~50% softer than CTCs (stiffness 8.8 kPa *versus* 16.6 kPa) but the other was almost seven times stiffer than CTCs (126 *versus* 16.6 kPa) (Fig. 1B). Dead and dying cells are stiff, so the stiff population of UPCs may have represented cells already undergoing apoptosis. High softness and low adhesion are known mesenchymal hallmarks of aggressive cancer cells, and the soft, non-adhesive class of UPCs embodied these traits. However, the majority of CTCs retained epithelial adhesion. This result suggests that CTCs display hybrid traits that maintain high cell adhesion to enable protective clustering and attachment to vessel walls for extravasation (22,34). At the same time the CTCs display mesenchymal properties for softness that may facilitate their adaptation to shear force stress in the blood circulatory system. Consistently, high adhesion and softness, were distinctive features of the most aggressive prostate cancer CTCs in our previous studies (16).

Both CTCs and UPCs are shed from the tumor; however only CTCs displayed the unique nanomechanical phenotype, presumably promoting their survival. CTCs may originate from

metastatic sites, not only the primary tumor as assumed for UPCs (1). Only two out of ten patients used for this study were diagnosed with distant spread (Table 1) and phenotypes of their CTCs did not belong to a separate class in the population of all CTCs (not shown in Fig. 1B; see also Supplementary Table S2). In a search for other features distinguishing blood-isolated and urine-isolated cells we turned our attention to immune cells accompanying UPCs and CTCs. Both blood filtrates and urine sediments contained large cells positive for epithelial marker EpCAM (epithelial cell adhesion molecule) but also numerous cells positive for pan-leukocyte marker CD45 (leukocyte common antigen) and $EpCAM^-$ (Supplementary Fig. S1A). We subjected a random sample of light/fluorescent microscope images of these cells to morphometric analysis of the cells footprint. As expected, blood filtrates were devoid of small cells that passed through the filter pores. $EpCAM^+$ cells were expectedly large in both blood and urine preparations. Their footprints corresponded to square cells with average lengths of 24 µm (44 CTCs; range of lengths 10 µm – 32 µm) or 21 µm (51 UPCs; range of lengths 8 µm – 30 µm), well within morphological parameters reported for CTCs (27). As expected, population of CTCs with larger footprints was more numerous than a similar population in UPCs (Fig. 1C). This may reflect the high content of CTC pairs in blood filtrates, consistent with high adhesiveness of CTCs as compared to UPCs. Such cell pairs are often poorly distinguishable from single cells in light microscope images, and are customarily counted as single objects in FDA-approved diagnostic/prognostic enumerations of CTCs. In turn, footprints of the immune cells found in urine sediments were rather small (50 cells; average diameter 10 µm, range 6 µm – 18 µm; Fig. 1C) corresponding to typical leukocytes with expected diameters ranging from 7 µm to 15 µm (35). Instead, 40 blood-derived $EpCAM^-CD45^+$ cells had an average diameter of 23 µm, (range: 16 µm – 25 µm; Fig. 1C). The observed difference in size distribution could not be attributed solely to the expected enrichment of blood filtrates in large cells. In 30 images of cells in urine sediments from 9 patients there were 51 $EpCAM^+CD45^-$ cells and 50 $EpCAM^-CD45^+$ cells. From among 40 images of blood filtrates (n = 20 patients) analyzed there were 44 $EpCAM^+CD45^-$ cells and 40 $EpCAM^-CD45^+$ cells. Notably, partitions of tumor-to-immune cells were very similar in preparations recovered from the two liquid biopsies, however large immune cells were absent in urine.

CTCs are accompanied by immune cells bearing surface markers of macrophages.

The exceptionally large immune cells co-purifying with CTCs may have corresponded to products of differentiation and polarization of monocytes, especially to macrophages (27). We designated all cells isolated by microfiltration as “tumor associated circulating cells” (TACCs) and attempted to classify them. The presence of TACCs was unique for the blood of cancer patients: filtration of the blood sample of a healthy donor turned our neither immune nor epithelial-like cells,

with scarce fragments of exfoliated vessel lining cells as the only filter-bound material (data not shown). We chose the following surface markers to characterize TACCs: epithelial marker EpCAM, EMT-indicating vimentin (36), macrophage scavenger receptor CD163 expressed by anti-inflammatory macrophages of M2 type of polarization, and the marker of M1 pro-inflammatory macrophages, the T-lymphocyte activation antigen CD80 (37). According to immunocytochemical clues, we classified the presumably tumor-derived cells as $EpCAM^+$ CTCs ($EpCAM^+$/$vimentin^{+/-}$/ immune $markers^-$) or EMT-CTCs ($EpCAM^-$/$vimentin^+$/immune $markers^-$) (Fig. 1D, S1B). CTCs were sometimes found in clusters with other CTCs (homogenous, in short "homo-clusters") or with immune cells (heterogeneous, "hetero-clusters"; Fig. 1D). In turn, the non-CTC TACCs presented macrophage-like signatures and could be assigned as M1-like macrophages ($EpCAM^-$/$vimentin^-$ /$CD163^-$/$CD80^+$), "intermediate" macrophages ($EpCAM^-$/$vimentin^-$/$CD163^+$/$CD80^+$) and M2-like macrophages ($EpCAM^-$/$vimentin^-$/$CD163^+$/$CD80^-$) (Supplementary Fig. S1,1D). The CD163 surface marker that was prominent in immune TACCs is commonly found on cancer-promoting tumor associated macrophages (TAMs) (38–40). TAMs serve as an important component of tumor microenvironment with immunoprotective, pro-angiogenic and invasiveness-supporting actions (40). Although usually referred as M2-like, TAMs often defy the canonical M1 – M2 polarization axis. The $CD163^+CD80^+$ signature referred here as "intermediate" may indicate TAMs of M2d-like type (40–42). TAMs may also display M1-like phenotype with detectable CD80 surface marker, raising the possibility that macrophages co-purifying with CTCs are circulation-born TAMs (43).

Mechanical fitness of CTCs correlates with enumeration of TAM-like immune cells.

To track possible links between nanomechanical phenotypes and the presence of distinctive macrophages, we performed a comprehensive mechanical and immunocytochemical analysis of TACCs isolated from 33 blood samples obtained from high-risk prostate cancer patients (n=23) with local disease or with low metastatic tumor burden, undergoing diverse treatments (e.g., prostatectomy, androgen deprivation therapy/ADT and chemotherapy) (Table 1). Two blood samples obtained during two separate visits at least several months apart were analyzed for nine patients. For select patients, clinical information was updated based on changes in castration sensitivity or development of metastasis several months after the initial visit (Table 1). The total of 514 single $EpCAM^+$ or $vimentin^+$ CTCs were interrogated with AFM. The filter-retained 4127 TACCs were analyzed with immune staining (Fig. 1D, Supplementary Fig. S1B). The results of nanomechanical profiling are presented in Fig. 2 and Supplementary Table S2). Hierarchical cluster analysis followed by principal component analysis (PCA) was used to identify four classes of CTCs distinguished by their nanomechanical phenotypes: 1 - extreme stiffness, 2 – moderate stiffness, deformability and adhesion, 3 – exceptionally soft (very low stiffness, very high deformability), 4 –

exceptionally adhesive (Fig. 2A). Then, we determined the partition of each class for all patients' CTC samples. From our previous study, softness and adhesion were deemed hallmarks of CTCs in prostate cancer patients with the most aggressive disease (16). On this basis, we ordered the samples according to contribution of "best fit" classes 4 and 3, from lowest to highest contribution. Next, we aligned the partition (Fig. 2B) and enumeration (Fig. 2C, Supplementary Fig. S2) of distinct kinds of TACCs with this "fitness chart" of patients' CTCs. Enumeration of $EpCAM^+$ CTCs generally decreased with increasing fitness (Fig. 2C), with no clear trend for enumeration of EMT CTCs (Supplementary Fig. S2). Enumeration of total TACCs, M1-like, intermediate as well as total macrophages increased with increasing fitness of CTCs, with no clear trend for enumeration of M2-like macrophages (Fig. 2C, Supplementary Fig. S2). When partition of distinct TACCs were considered, decreasing contribution of $EpCAM^+$ CTCs and increasing contribution of total macrophages with increasing fitness of CTCs were apparent (Fig. 2B).

In a search for formal representation of the trends we turned to general linear regression analysis. We translated the partition of mechanical phenotype classes (Fig. 2A, B) into enumeration of the classes in the total CTC population. The strongest correlations are presented in Figure 3 and Supplementary Figure S3. Apparently, enumeration of class 3 with well-fit, very soft cells (Fig. 2A) correlated with enumeration of intermediate macrophages (Fig. 3A). In turn, enumeration of class 2 with moderately fit cells (Fig. 2A) correlated with enumeration of M2-like macrophages (Fig. 3B). We may speculate that cells from this category were coached specifically by M2-like macrophages to attain fitness. Enumeration of well-fit, soft and very adhesive cells from category 4 (Fig. 2A) only weakly correlated with enumeration of M1-like (Supplementary Fig. S3A) and intermediate macrophages (Supplementary Fig. S3B). Possibly these CTCs were already in sufficiently good condition and did not strongly rely on the presence of macrophages for survival. Enumeration of the poorly fit category 1 (very stiff cells; Fig. 2A) did not significantly correlate with any macrophage enumerations (data not shown). These cells were likely destined for apoptosis without evidence of positive or negative intervention from macrophages.

Next, we attempted to search for patterns of clinical conditions (clinicopathology, treatment history) in our CTCs fitness chart. Apparently, CTCs isolated from patients that never underwent hormonal therapy (pre-ADT) tended to display rather low or moderate fitness (Fig. 2B). This trend was supported by a cluster analysis of nanomechanical parameters and enumerations of TACCs as variables: a separate cluster was formed by pre-ADT cases with one exception: case No. 2 was analyzed only 3 months following the initiation of ADT (Supplementary Fig. S4, Table 1). Another striking finding was that the nine patients in this cluster were all castration sensitive and this was confirmed for all of them during their follow-up visits (Supplementary Fig. S4, Table 1). With the

exception of patient No. 10, there was no distant spread evident in the other castrate sensitive patients (Supplementary Fig. S4, Table 1).

To understand the effects of ADT treatment on CTCs, we compared the nanomechanical parameters and enumerations of TACCs from patients before and after ADT treatments (Fig. 3C and D). Deformability (a hallmark of circulating cells) strongly positively correlated with enumeration of intermediate macrophages in both pre- and post-ADT treatment samples. Adhesion, in turn, especially strongly and positively correlated with enumeration of M1 and intermediate macrophages in pre-ADT cases (Fig. 3C). Stiffness negatively correlated with enumeration of M2-like macrophages in pre-ADT treatment samples and weakly correlated with enumeration of intermediate macrophages following ADT treatment samples (Fig. 3C). Low stiffness was commonly observed in well-fit CTCs (Fig. 2A). Next, we considered correlations between enumeration parameters. Enumeration of CTC EMT positively correlated with number of clustered CTCs and M2-like macrophages, the latter for both pre-and post-ADT cases (Fig. 3D). When it comes to enumeration of macrophages, the strongest positive correlations were observed between intermediate and M1-like macrophages and (weaker) intermediate and M2 macrophages in post-ADT cases (Fig. 3D). Intermediate macrophages might be expected to cluster with pre-ADT CTCs taking into account the respective positive correlation (Fig. 3D). Ominously, enumeration of $EpCAM^+$ CTCs only weakly correlated with enumerations of other TACCs (Fig. 2C, Supplementary Fig. S4). The occasionally observed negative correlations between macrophage enumeration and enumeration of hetero-clusters may indicate that numerous clusters were broken during isolation of TACCs. Taken together, the aggressive nanomechanical phenotypes of well-fit CTCs were accompanied by high enumeration of macrophages, particularly in patients who were not previously treated with ADT.

The status of ADT and status of castration sensitivity were not the only clinical parameters trending with mechanical fitness of CTCs or enumeration of TACCs. The order of cases in CTCs fitness chart did not follow the reported metastatic spread, as cases with localized disease or distant metastases were widely distributed (Supplementary Fig. S2). Instead, we focused on adhesion as the most distinctive parameter distinguishing CTCs from tumor-shed cells such as UPCs. Next, we performed binary logistic regression using the average adhesion of CTCs for each patient and their corresponding disease spread status (Table 1, Supplementary Table S2). We noticed a correlative trend ($p=0.22$) in high cell adhesion with metastasis. We posit that the increase in CTC adhesion may portend a poor prognosis with higher risk for development of metastasis. Importantly, other mechanical parameters did not show any such trend. This observation underscored a special significance of cell adhesion for the mechanical fitness and presumed survival skills, resilience and ultimately invasiveness of CTCs.

Cultured prostate cancer cells respond to co-culture with model macrophages with improved mechanical fitness.

To recapitulate the putative productive interactions between tumor cells and macrophages, we turned to cell culture models. We chose three prostate cancer cell lines of distinct invasiveness. The moderately invasive 22Rv-1 cell line derived from androgen sensitive xenograft of primary tumor cells bear androgen receptor splice variants with diverse androgen sensitive or independent profiles. The poorly invasive brain-metastasis derived DU145 cells are androgen receptor-negative and androgen independent. The highly invasive C4-2 cells derived from LNCaP cell line express mutated androgen receptor and are androgen independent. The cells cultured alone displayed diverse nanomechanical profiles, as demonstrated in Figure 4. Comparison of 40 22Rv1, 47 DU145 and 52 C4-2 cells with 514 CTCs (total 653 cells) revealed that at least subsets of these cultured cells were very similar to CTCs in terms of their nanomechanical phenotypes. The primary tumor-derived 22Rv1 cells most closely resembled CTCs (Fig. 4A). The spread of all parameters in control 22Rv1 cells was the largest, likely due to their mixed genetic background (Fig. 4B). In turn, high adhesion, about 1000 nN on average, was the most distinctive feature of DU145 cells, as it was more than twice as high as adhesion of 22Rv1 or C4-2 cells (averages about 400 nN; Fig. 4C). C4-2 cells were soft and not very adhesive, suggesting mesenchymal-like phenotype expected in highly invasive tumor cells (Fig. 4D). When cells from each of the lines were separately categorized into four classes according to mechanical fitness, 22Rv1 cells had approximately equal representation of classes with low to high relative fitness (Fig. 5A), in DU145 cells the moderate-fitness class prevailed (Fig. 5B), whereas majority of tested C4-2 cells were highly fit in terms of softness, however moderately prepared for potential cell-cell interactions (Fig. 5C). In summary, cultured cells presented nanomechanical profiles comparable to CTCs, albeit more extreme than majority of CTCs: 22Rv1 cells and C4-2 cells were softer, whereas DU145 cells were more adhesive than patient-isolated cells (Fig. 4A). Such diversity of nanomechanical profiles positioned these cultured cell lines as good models representing prostate cancer cells spanning different clinical stages of propensity for metastatic tumor spread.

In the next series of experiments, we co-cultured the model prostate cancer cells for 24 hours with *in vitro* differentiated and polarized model human macrophage-like cells derived from monocytic U937 cell line. All three cancer cell lines were expressing GFP for unequivocal identification of prostate cells in co-culture. We used differentiated, non-polarized M0-like naïve macrophages; M1-like polarized or M2-like polarized U937-derived macrophages in a 1:1 ratio with cancer cells. Single cancer cells were phenotyped with AFM, as in the above-described control experiments, adding 277 cells to the analysis. Apparently, co-culture with all types of model

macrophages affected nanomechanical profiles of prostate cancer cells; however extent and direction of changes depended both on the polarization of immune cells and the cancer cell line (Fig. 4). The phenotypes of 22Rv1 cells were affected the most by M2-like macrophages, with significantly softer but less adhesive cells after co-culture (Fig. 4A, 5B). The class 4 of stiff cells disappeared entirely from co-cultures with M2-like macrophages. Co-culture with M0 and M1-like macrophages was accompanied by a moderately increased participation of soft and adhesive cells (Fig. 5A). Interestingly, co-culture with M1-like macrophages was accompanied by the most pronounced changes in nanomechanical phenotype of DU145 cells: classes of very soft as well as soft and adhesive cells prevailed (Fig. 4C, 5B). Still, adhesion of tumor cells systematically increased with not only M1- but also M0- and M2-like macrophages as partners in co-culture (Fig. 5B). In turn, the C4-2 cells responded similarly to the presence of all types of macrophages: a sizable fraction of cells retained high softness and attained higher adhesion (Fig. 4D, 5C). Accordingly, both adhesion and deformability increased significantly after co-culture with M0-, M1- and M2-like macrophages (Fig, 4D). In general, co-culture with polarized macrophages seemed to have more pronounced effects on nanomechanical phenotypes than co-culture with naïve macrophages (Supplementary Fig. S7A-C). Comparison of nanomechanical parameters of patient-isolated CTCs and model cultured cells confirmed that co-culture with model macrophages consistently promoted fitness: high adhesion, high deformability and low stiffness, with majority of 22Rv1 and C4-2 cells still remaining within the range of the mechanical similarity to CTCs (Supplementary Fig. S7D).

Co-culture of DU145 cells with macrophages results in hybrid EMT proteomic profile.

To understand molecular mechanisms that promote changes in nanomechanical phenotype we conducted proteomic analysis using DU145 cell line co-culture model. These cells responded to co-culture with macrophages with the most pronounced AFM-detected shifts (Fig. 4 and 7, Supplementary Fig. S5). GFP-DU145 cultured alone (control) or with M0, M1 or M2- model macrophages were separated from immune cells in Cytobank and subjected to cytometry by time-of flight (CyTOF) with epithelial/mesenchymal panel of 16 antibodies (Fig. 6A-C, Supplementary Table S2). t-Distributed Stochastic Neighbor Embedding (t-SNE) projections of treatments of DU145 cells are presented in Figure 6B. Each of four treatment-populations was further divided into subpopulations with distinct proteomic marker profiles for eight mesenchymal and seven epithelial markers (Fig. 6B). As evident in Figure 6C, the cells expressed both epithelial and mesenchymal markers. For example, in control cells high levels of mesenchymal β-catenin, vimentin, N-cadherin and Slug were accompanied by high levels of epithelial EpCAM, cytokeratins (CK) 8/18 and ZO2. This profile remained mixed EMT/epithelial after co-cultures with macrophages: levels of selected

epithelial and mesenchymal markers still remained high (Fig. 6C). However, cumulative analysis revealed that contribution of mesenchymal markers systematically decreased upon co-culture with macrophages, with polarized macrophages triggering stronger shifts than M0-like immune cells (Fig. 6D and E). These changes mirrored those in nanomechanical phenotype of DU145 cells, where co-culture with M1- and M2-like macrophages introduced stronger fitness-promoting trends than naïve M0 macrophages (Fig. 4C, 7B). Apparently, the mechanical fitness beneficial for CTC survival was supported by a partial reversion from an advanced mesenchymal to a more-epithelial phenotype. A striking example of reversion is a decreasing level of TWIST and N-cadherin accompanied by increasing level of E-cadherin in DU145 cells co-cultured with M2 macrophages (Fig. 6C). In the course of standard EMT TWIST is repressing transcription of E-cadherin (44). Contribution of oncogenic signal components followed the hybrid EMT/epithelial profile as well: certain markers such as VEGFR1 or Wnt5a were at the highest in control DU145 cells, however some others, most notably SMAD2, EGFR and P-ERK1/2 attained high levels in the co-cultured cells (Fig. 6F). It seems that cancer cells educated by macrophages may forgo certain features of invasive mesenchymal phenotype in favor of hybrid EMT promoting mechanical endurance especially important for CTCs in circulation. Maintaining the high adhesion and high softness appears to be the most distinctive manifestation of CTC-relevant hybrid EMT.

DISCUSSION

Mechanical phenotypes of cells are tuned with their physiological function: rigidity of osteocytes, and deformability of erythrocytes providing examples of extreme adaptations (45). Changes in mechanical phenotypes are often very early and sensitive signs of physiological changes in the tissue environment (18,46). Not surprisingly, tumor cells turn mechanical properties to their advantage. Prostate tumor, as other epithelial-origin tumors, is an overcrowded structure. Inhabitant cells are mechanically labile to survive the inter-tumor pressure and many cells readily escape the tumor. The escapees may be a random set of cells that happened to be positioned close to the outside routes: the urethra, the lymph vessels or the blood vessels. Alternatively, the cells may be uniquely prepared for dissemination. Here we compared mechanical phenotypes of prostate tumor cells shed to urine (UPCs) and to blood (CTCs). Both cell populations experience fluid shear stress of similar magnitudes when comparing liquid flow in urethra and veins (47–49), however, we found their mechanical phenotypes to be strikingly different. Mechanical properties of soft and non-adhesive UPCs expectedly reflected their aggressive tumor origin, whereas CTCs were distinguished by high adhesion, a feature not associated with invasive tumor resident cells but found in exceptionally aggressive CTCs (16). A sizable number of UPCs were stiff, presumably damaged by urine flow. We did not detect such cells among CTCs. We concluded that while UPCs

represent a random sample of tumor cells, the CTCs might be specifically equipped for dissemination. Since only CTCs co-purified with large numbers of immune cells bearing markers of TAMs, we hypothesized that tumor-escaping CTCs and TAMs are uniquely linked for promotion of metastatic spread.

In a search for putative connection between aggressive traits of CTCs and the presence of macrophages, we analyzed the nanomechanical phenotypes of the CTCs and compared them with abundance of the macrophages. Following our previous works with prostate cancer CTCs we considered elevated softness and adhesion as biomarkers of aggressive disease and hallmarks of survival-promoting mechanical fitness (16). We found enumeration and abundance of $EpCAM^+$ CTCs to be low in samples with the best-fit cells. This pointed at a shortcoming of affinity-based CTC isolation methods that neglect EMT-undergoing $EpCAM^-$ cells than actually may be best equipped for metastatic spread. Importantly, we observed trends linking high abundance of CTCs with aggressive mechanical phenotype with high enumeration of all co-purified macrophages. Preferences of CTCs with particular nanomechanical phenotypes to co-isolate with macrophages of certain polarizations may point at mechanisms of protecting and coaching CTCs to advance EMT and enhance metastatic potential. We also noted a similar association of CTCs nanomechanics and enumeration of macrophages in blood samples isolated from liver, pancreatic and lung cancers (unpublished observations).

We did not detect a substantial correlation between mechanical fitness of CTCs and PSA levels or Gleason scores, consistently with our previous studies on castration sensitive and resistant patients (16). In the cohort analyzed in this study over 90% of cases were labeled as castration-sensitive at the time of the blood draw. However, the patients displayed diverse history of ADT. CTCs isolated from post-ADT patients, even those responding to AD, were generally well fit, likely reflecting the long course of disease in these patients. The pronounced differences between pre- and post-ADT cases highlight necessity of tailoring different therapeutic approaches. Interestingly, the presumed relations between CTCs and macrophages seemed to be more pronounced in pre-ADT than in post-ADT cases, as suggested by the strong correlations between mechanical parameters and TACCs enumeration. The correlations point at possible predictive clues that we pursue vigorously. For now, we have longitudinal data with clinical outcomes available for less than half of the patients (11 out of 23). However, the data are encouraging: mechanical phenotypes and enumerations of TACCs isolated from patients that remained CS tend to cluster together. The predictive potential of TACCs phenotyping may be understandably limited to several months. For example, in the case of patient No. 7-8 the phenotyping indicated rather poorly fit CTCs during first (No. 7; start ADT) and second (No. 8; 6 months later) visits, correctly predicting castration sensitivity. However, more than a year later, after additional treatments and another round of ADT

the patient was diagnosed with castration resistance. One might speculate that a relatively large advance of mechanical phenotype toward higher fitness between visit 1 and 2 in this case indicated the future failure of therapy – an observation worthy of further exploration. Apart from castration resistance, our observation suggesting a trend linking high adhesion of CTCs with the presence of metastatic disease may bear a significant prognostic potential to be explored with longitudinal studies.

The correlations observed for patient-isolated TACCs obviously did not implicate causative relationships. However, our analysis of prostate cancer cells co-cultured with model macrophages strongly suggested that macrophages might instruct cancer cells to acquire mechanical fitness. Interestingly, it was reported that macrophages may respond to mechanical clues in a similar manner to canonical ligand-receptor stimuli (50). This opens a possibility of functionally relevant mechanical cross-influence of both types of cells. The stationary conditions selected for co-culture did not include fluid shear stress and thus corresponded to a pre-intravasation stage of the future-CTC's life. Polarized macrophages rather than M0-like naïve cells were linked to most significant shifts in mechanical phenotypes pointing at specificity of cancer cells-immune cells interactions. The strongest shift observed in the co-culture model with polarized macrophages was an increase in cancer cells' adhesion in an apparent partial reversal of EMT also detected in patient-isolated CTCs. The sole exception with a significant decrease in adhesion was observed for 22Rv1 cells co-cultured with M2-like macrophages. 22Rv1 cells are considered the most diverse and relatively least-fit among the model cells analyzed. The cells may use the specific macrophage-mediated boost to proceed with EMT, increase softness and decrease adhesion before the CTC-specific partial EMT reversal. The partial reversal of EMT in model tumor cells co-cultured with macrophages was confirmed by proteomic studies. The reversal was apparent with both non-polarized and polarized macrophages, however mesenchymal and epithelial markers responded distinctly to particular types of macrophages, possibly signaling multiple stages of hybrid EMT. The context-dependent plasticity of cancer-relevant processes under the broad term hybrid EMT is increasingly being acknowledged, including its importance for CTC invasiveness (12,14,15,51,52). In turn, enhanced adhesive properties of cancer cells have been recently recognized as crucial for efficient cell survival and dissemination (53,54). Our data add to the notion of EMT plasticity and diversity and point at the mechanical phenotype as the robust functional readout aligned with the cancer cells' destiny.

Multiple observations from patient-isolated tumor-associated circulating cells, animal models and cell cultures support the metastasis-promoting role of TAMs (3,40,55,56). Indeed, the induction of EMT in tumor cells by TAMs have been described before (55,56). Moreover, TAMs have been noted to actively help tumor cells to traverse endothelial barrier during intravasation (3,57,58). We

demonstrate that specific modulation of mechanical properties is the critical part of TAM-CTC relationship.

Here we propose that TAMs coach selected tumor cells to reach a distinctive stage of EMT characterized by high softness and high adhesion, with a mix of epithelial and mesenchymal molecular markers. Selection of tumor cells can be based in part on mechanical cues affecting cells subjected to in-tumor pressure (Qian, Osmulski, Gaczynska, unpublished observations). The hybrid EMT/mechanical fitness phenotype is critical for early survival of CTCs. Adhesive CTCs may intravasate as large clusters called circulating tumor microemboli (CTMs), which gives them a survival advantage (3,13). TAMs may accompany CTCs and continue to help them as a part of CTMs or smaller clusters. An extreme form of assistance from macrophages would be formation of invasive CTC-macrophage fusions (59). Among the diverse microfiltration-isolated TACCs we noted putative fused cells, positive for both tumor cell and immune cell markers, not included in our enumerations. The phenomenon beyond the scope of this study is open for future exploration. The adhesive CTCs may also recruit other cells for support, including aid with extravasation. For example, platelets abundant in the blood may coat CTCs, shield them from shear stress and natural killer cells attacks, promote EMT and finally support extravasation (24). In turn, myeloid derived suppressor cells (MDSCs) found in tumor environment and in circulation (60–62), can cluster with CTCs, protect them from immune cells and promote mitogenesis (25). In turn, CTC-neutrophil interactions lead to cell cycle progression and also stimulate interactions with endothelial cells for extravasation (26,63).

Summarizing our and others data from the life journey of CTCs we envision the following metastasis-promoting chain of events. TAMs train CTCs for mechanical endurance and propensity to cluster, help them to intravasate and accompany them as chaperones in the blood. CTCs use the high adhesiveness to keep integrity of microemboli and for abundant cell-cell interactions. All cells clustered with CTCs act as shields from fluid shear stress and leukocyte attacks. Platelets, MDSCs and neutrophils additionally help in later stages of CTCs life re-starting EMT and proliferation and enabling extravasation. This chain of events from intra- to extravasation and metastatic growth would not be possible without the macrophage – promoted hybrid EMT and mechanical fitness of CTCs.

Acknowledgements

This work was supported by DoD grant PC170821 and NIH U54 CA217297-01. The Authors acknowledge the assistance of the Bioanalytics and Single-Cell Core (BASiC) for atomic force microscopy and mass cytometry studies, in part supported by the Cancer Prevention and Research Institute of Texas (CPRiT) award RP150600.

References

1. Micalizzi DS, Maheswaran S, Haber DA. A conduit to metastasis: circulating tumor cell biology. Genes Dev. 2017;31(18):1827–40.
2. Gorges TM, Pantel K. Circulating tumor cells as therapy-related biomarkers in cancer patients. Cancer Immunol Immunother. 2013;62(5):931–9.
3. Katt ME, Wong AD, Searson PC. Dissemination from a Solid Tumor: Examining the Multiple Parallel Pathways. Trends in Cancer. 2018 Jan;4(1):20–37.
4. Jin K, Chen X, Lan H, Wang S, Ying X, Abdi SM, et al. Current progress in the clinical use of circulating tumor cells as prognostic biomarkers. Cancer Cytopathol. 2019 Dec 7;127(12):739–49.
5. Bitting RL, Schaeffer D, Somarelli JA, Garcia-Blanco MA, Armstrong AJ. The role of epithelial plasticity in prostate cancer dissemination and treatment resistance. Cancer Metastasis Rev. 2014;33(2):441–68.
6. Gorges TM, Tinhofer I, Drosch M, Röse L, Zollner TM, Krahn T, et al. Circulating tumour cells escape from EpCAM-based detection due to epithelial-to-mesenchymal transition. BMC Cancer. 2012;12.
7. Stroka KM, Konstantopoulos K. Physical Biology in Cancer. 4. Physical cues guide tumor cell adhesion and migration. AJP Cell Physiol. 2014 Jan;306(2):C98–109.
8. Savagner P. The epithelial-mesenchymal transition (EMT) phenomenon. Ann Oncol. 2010;21(SUPPL. 7):vii89-vii92.
9. Chen CL, Mahalingam D, Osmulski P, Jadhav RR, Wang CM, Leach RJ, et al. Single-cell analysis of circulating tumor cells identifies cumulative expression patterns of EMT-related genes in metastatic prostate cancer. Prostate. 2013;73(8):813–26.
10. Yang Y-J, Kong Y-Y, Li G-X, Wang Y, Ye D-W, Dai B. Phenotypes of circulating tumour cells predict time to castration resistance in metastatic castration-sensitive prostate cancer. BJU Int. 2019 Aug;124(2):258–67.
11. Lecharpentier A, Vielh P, Perez-Moreno P, Planchard D, Soria JC, Farace F. Detection of circulating tumour cells with a hybrid (epithelial/mesenchymal) phenotype in patients with metastatic non-small cell lung cancer. Br J Cancer. 2011/10/04. Nature Publishing Group; 2011 Oct 25;105(9):1338–41.
12. Pastushenko I, Brisebarre A, Sifrim A, Fioramonti M, Revenco T, Boumahdi S, et al. Identification of the tumour transition states occurring during EMT. Nature. 2018;556(7702):463–8.
13. Aceto N, Bardia A, Miyamoto DT, Donaldson MC, Wittner BS, Spencer JA, et al. Circulating Tumor Cell Clusters Are Oligoclonal Precursors of Breast Cancer Metastasis. Cell. Elsevier

Inc.; 2014;158(5):1110–22.
14. Williams ED, Gao D, Redfern A, Thompson EW. Controversies around epithelial–mesenchymal plasticity in cancer metastasis. Nat Rev Cancer. 2019;19(12):716–32.
15. Liao T-T, Yang M-H. Hybrid Epithelial/Mesenchymal State in Cancer Metastasis: Clinical Significance and Regulatory Mechanisms. Cells. MDPI; 2020 Mar 4;9(3):623.
16. Osmulski P, Mahalingam D, Gaczynska ME, Liu J, Huang S, Horning AM, et al. Nanomechanical biomarkers of single circulating tumor cells for detection of castration resistant prostate cancer. Prostate. 2014;74(13).
17. Cross SE, Jin Y-S, Rao J, Gimzewski JK. Nanomechanical analysis of cells from cancer patients. Nat Nanotechnol. 2007;2(12):780–3.
18. Lekka M. Discrimination Between Normal and Cancerous Cells Using AFM. Bionanoscience. 2016 Mar 30;6(1):65–80.
19. Rejniak KA. Investigating dynamical deformations of tumor cells in circulation: predictions from a theoretical model. Front Oncol. 2012;2.
20. Mohamed H, Murray M, Turner JN, Caggana M. Isolation of tumor cells using size and deformation. J Chromatogr A. 2009 Nov;1216(47):8289–95.
21. Lamouille S, Xu J, Derynck R. Molecular mechanisms of epithelial–mesenchymal transition. Nat Rev Mol Cell Biol. 2014 Feb;15(3):178–96.
22. Huang G, Osmulski PA, Bouamar H, Mahalingam D, Lin C-L, Liss MA, et al. TGF-β signal rewiring sustains epithelial-mesenchymal transition of circulating tumor cells in prostate cancer xenograft hosts. Oncotarget. 2016;7(47).
23. Heeke S, Mograbi B, Alix-Panabières C, Hofman P. Never Travel Alone: The Crosstalk of Circulating Tumor Cells and the Blood Microenvironment. Cells. 2019 Jul 13;8(7):714.
24. Leblanc R, Peyruchaud O. Metastasis: new functional implications of platelets and megakaryocytes. Blood. 2016;128(1):24–31.
25. Sprouse ML, Welte T, Boral D, Liu HN, Yin W, Vishnoi M, et al. PMN-MDSCs Enhance CTC Metastatic Properties through Reciprocal Interactions via ROS/Notch/Nodal Signaling. Int J Mol Sci. 2019 Apr 18;20(8):1916.
26. Szczerba BM, Castro-Giner F, Vetter M, Krol I, Gkountela S, Landin J, et al. Neutrophils escort circulating tumour cells to enable cell cycle progression. Nature. 2019 Feb 6;566(7745):553–7.
27. Adams DL, Martin SS, Alpaugh RK, Charpentier M, Tsai S, Bergan RC, et al. Circulating giant macrophages as a potential biomarker of solid tumors. Proc Natl Acad Sci U S A. 2014;111(9):3514–9.
28. Chen M, Pereira-Smith OM, Tominaga K. Loss of the chromatin regulator MRG15 limits

neural stem/progenitor cell proliferation via increased expression of the p21 Cdk inhibitor. Stem Cell Res. 2011 Jul;7(1):75–88.

29. Marie Genin, Francois Clement, Antoine Fattaccioli MR and CM. M1 and M2 macrophages derived from THP-1 cells differentially modulate the response of cancer cells to etoposide. BMC Cancer. 2015;15:577.
30. Hsu Y-T, Osmulski P, Wang Y, Huang Y-W, Liu L, Ruan J, et al. EpCAM-regulated transcription exerts influences on nanomechanical properties of endometrial cancer cells that promote epithelial-to-mesenchymal transition. Cancer Res. 2016;76(21).
31. Sokolov I, Dokukin ME, Guz N V. Method for quantitative measurements of the elastic modulus of biological cells in AFM indentation experiments. Methods. Elsevier Inc.; 2013;60(2):202–13.
32. Iyer S, Gaikwad RM, Subba-Rao V, Woodworth CD, Sokolov I. Atomic force microscopy detects differences in the surface brush of normal and cancerous cells. Nat Nanotechnol. 2009 Jun 12;4(6):389–93.
33. Truong M, Yang B, Jarrard DF. Toward the Detection of Prostate Cancer in Urine: A Critical Analysis. J Urol. 2013 Feb;189(2):422–9.
34. Sarioglu AF, Aceto N, Kojic N, Donaldson MC, Zeinali M, Hamza B, et al. A microfluidic device for label-free , physical capture of circulating tumor cell clusters. 2015;12(7).
35. Downey GP, Doherty DE, Schwab B, Elson EL, Henson PM, Worthen GS. Retention of leukocytes in capillaries: role of cell size and deformability. J Appl Physiol. 1990 Nov 1;69(5):1767–78.
36. Armstrong AJ, Marengo MS, Oltean S, Kemeny G, Bitting RL, Turnbull JD, et al. Circulating tumor cells from patients with advanced prostate and breast cancer display both epithelial and mesenchymal markers. Mol Cancer Res. 2011;9(8):997–1007.
37. Ambarus CA, Krausz S, van Eijk M, Hamann J, Radstake TRDJ, Reedquist KA, et al. Systematic validation of specific phenotypic markers for in vitro polarized human macrophages. J Immunol Methods. 2012 Jan;375(1–2):196–206.
38. Shabo I, Stål O, Olsson H, Doré S, Svanvik J. Breast cancer expression of CD163, a macrophage scavenger receptor, is related to early distant recurrence and reduced patient survival. Int J Cancer. 2008 Aug 15;123(4):780–6.
39. Cao W, Peters JH, Nieman D, Sharma M, Watson T, Yu J. Macrophage subtype predicts lymph node metastasis in oesophageal adenocarcinoma and promotes cancer cell invasion in vitro. Br J Cancer. 2015 Sep 11;113(5):738–46.
40. Lin Y, Xu J, Lan H. Tumor-associated macrophages in tumor metastasis: biological roles and clinical therapeutic applications. J Hematol Oncol. 2019 Dec 12;12(1):76.

41. Shrivastava R, Shukla N. Attributes of alternatively activated (M2) macrophages. Life Sci. 2019 May;224:222–31.
42. Wang Q, Ni H, Lan L, Wei X, Xiang R, Wang Y. Fra-1 protooncogene regulates IL-6 expression in macrophages and promotes the generation of M2d macrophages. Cell Res. 2010 Jun;20(6):701–12.
43. Murray PJ. Macrophage Polarization. Annu Rev Physiol. 2017 Feb 10;79(1):541–66.
44. Li J, Alvero AB, Nuti S, Tedja R, Roberts CM, Pitruzzello M, et al. CBX7 binds the E-box to inhibit TWIST-1 function and inhibit tumorigenicity and metastatic potential. Oncogene. 2020;39(20):3965–79.
45. Luo Q, Kuang D, Zhang B, Song G. Cell stiffness determined by atomic force microscopy and its correlation with cell motility. Biochim Biophys Acta - Gen Subj. 2016;1860(9):1953–60.
46. Zemła J, Danilkiewicz J, Orzechowska B, Pabijan J, Seweryn S, Lekka M. Atomic force microscopy as a tool for assessing the cellular elasticity and adhesiveness to identify cancer cells and tissues. Semin Cell Dev Biol. 2018;73:115–24.
47. Ballermann BJ, Dardik A, Eng E, Liu A. Shear stress and the endothelium. Kidney Int. 1998;54:S100–8.
48. Deng Y, Papageorgiou DP, Chang H-Y, Abidi SZ, Li X, Dao M, et al. Quantifying Shear-Induced Deformation and Detachment of Individual Adherent Sickle Red Blood Cells. Biophys J. Elsevier; 2019 Jan 22;116(2):360–71.
49. Khismatullin DB. The cytoskeleton and deformability of white blood cells. 2009.
50. Patel NR, Bole M, Chen C, Hardin CC, Kho AT, Mih J, et al. Cell elasticity determines macrophage function. PLoS One. 2012;7(9):e41024.
51. Cook DP, Vanderhyden BC. Context specificity of the EMT transcriptional response. Nat Commun. 2020;11(1):2142.
52. Kröger C, Afeyan A, Mraz J, Eaton EN, Reinhardt F, Khodor YL, et al. Acquisition of a hybrid E/M state is essential for tumorigenicity of basal breast cancer cells. Proc Natl Acad Sci. 2019 Apr 9;116(15):7353 LP-7362.
53. Janiszewska M, Primi MC, Izard T. Cell adhesion in cancer: Beyond the migration of single cells. J Biol Chem . 2020 Feb 21;295(8):2495–505.
54. Kim H, Ishibashi K, Matsuo K, Kira A, Okada T, Watanabe K, et al. Quantitative Measurements of Intercellular Adhesion Strengths between Cancer Cells with Different Malignancies Using Atomic Force Microscopy. Anal Chem. American Chemical Society; 2019 Aug 20;91(16):10557–63.
55. Su S, Liu Q, Chen J, Chen J, Chen F, He C, et al. A Positive Feedback Loop between

Mesenchymal-like Cancer Cells and Macrophages Is Essential to Breast Cancer Metastasis. Cancer Cell. 2014 May;25(5):605–20.

56. Wei C, Yang C, Wang S, Shi D, Zhang C, Lin X, et al. Crosstalk between cancer cells and tumor associated macrophages is required for mesenchymal circulating tumor cell-mediated colorectal cancer metastasis. Mol Cancer. 2019 Dec 30;18(1):64.
57. Roussos ET, Condeelis JS, Patsialou A. Chemotaxis in cancer. Nat Rev Cancer. 2011;11(8):573–87.
58. Harney AS, Arwert EN, Entenberg D, Wang Y, Guo P, Qian B-Z, et al. Real-Time Imaging Reveals Local, Transient Vascular Permeability, and Tumor Cell Intravasation Stimulated by TIE2hi Macrophage-Derived VEGFA. Cancer Discov. 2015 Sep 1;5(9):932–43.
59. Gast CE, Silk AD, Zarour L, Riegler L, Burkhart JG, Gustafson KT, et al. Cell fusion potentiates tumor heterogeneity and reveals circulating hybrid cells that correlate with stage and survival. Sci Adv. 2018 Sep 1;4(9).
60. Porta C, Sica A, Riboldi E. Tumor-associated myeloid cells: new understandings on their metabolic regulation and their influence in cancer immunotherapy. FEBS J. 2018 Feb;285(4):717–33.
61. Yang L, Huang J, Ren X, Gorska AE, Chytil A, Aakre M, et al. Abrogation of TGFβ Signaling in Mammary Carcinomas Recruits Gr-1+CD11b+ Myeloid Cells that Promote Metastasis. Cancer Cell. 2008 Jan;13(1):23–35.
62. Du R, Lu K V., Petritsch C, Liu P, Ganss R, Passegué E, et al. HIF1α Induces the Recruitment of Bone Marrow-Derived Vascular Modulatory Cells to Regulate Tumor Angiogenesis and Invasion. Cancer Cell. 2008 Mar;13(3):206–20.
63. Spicer JD, McDonald B, Cools-Lartigue JJ, Chow SC, Giannias B, Kubes P, et al. Neutrophils Promote Liver Metastasis via Mac-1–Mediated Interactions with Circulating Tumor Cells. Cancer Res. 2012 Aug 15;72(16):3919–27.